molecular pharmaceutics



Article

# Fluorescent Penetration Enhancers Reveal Complex Interactions among the Enhancer, Drug, Solvent, and Skin

Monika Kopecna, Andrej Ková#ik, Ondrej Kucera, Miloslav Machacek, Michaela Sochorova, Pavla Audrlicka, and Katerina Vavrova

*Mol. Pharmaceutics*, **Just Accepted Manuscript** • DOI: 10.1021/acs.molpharmaceut.8b01196 • Publication Date (Web): 10 Jan 2019



## Just Accepted



ACS Publications

is published by the American Chemical Society. 1155 Sixteenth Street N.W., Washington, DC 20036

# Fluorescent Penetration Enhancers Reveal Complex Interactions among the Enhancer, Drug, Solvent, and Skin

Monika Kopečná,[a] Andrej Kováčik,[a] Ondřej Kučera,[a] Miloslav Macháček,[b] Michaela Sochorová,[a] Pavla Audrlická,[a] Kateřina Vávrová[a,*]

[a]Skin Barrier Research Group, Charles University, Faculty of Pharmacy in Hradec Králové, Heyrovského 1203, 50005 Hradec Králové, Czech Republic

[b]Department of Biochemical Sciences, Charles University, Faculty of Pharmacy in Hradec Králové, Heyrovského 1203, 50005 Hradec Králové, Czech Republic

*corresponding author: Kateřina Vávrová, Skin Barrier Research Group, Charles University, Faculty of Pharmacy in Hradec Králové, Heyrovského 1203, 50005 Hradec Králové, Czech Republic; E-Mail: katerina.vavrova@faf.cuni.cz. Tel.: +420 495 067 497. Fax: +420 495 067 166.

## ABSTRACT

Skin penetration/permeation enhancers facilitate drug delivery through the skin barrier. However, the specific mechanisms that govern the enhancer interactions with the skin, drug, and donor solvent are not fully understood. We designed and synthesized fluorescent-labeled enhancers by attaching 7-nitrobenzo[c][1,2,5]oxadiazol-4-yl (NBD) groups to 6-aminohexanoic acid esters. These NBD esters (applied at a 1% concentration) enhanced the permeation of the model drugs theophylline and hydrocortisone through human skin *in vitro* up to 6.6 and 3.9 times, respectively. The enhancement effects were strongly affected by the ester chain length (C8-C12) and the polarity of the donor solvent. Using HPLC with fluorescence detection, no NBD esters were detected in the acceptor buffer, but their hydrolysis product, NBD acid, was detected, whereas both acid and esters were found in the skin. The enhancer hydrolysis occurred in the lower *stratum corneum* and epidermis; the more hydrophilic NBD acid, which is an inactive enhancer, penetrated deeper. This illustrates the principle of biodegradable enhancers. The enhancer concentrations in the skin depended not only on the enhancer chain length and the donor solvent but also on the drug used. Thus, the drug, when co-applied with the enhancer, modulates the enhancer penetration into the skin and, consequently, its effect. Finally, active (NBD-C8 ester) and inactive (NBD acid) enhancers were visualized in human skin by confocal laser scanning microscopy. Both compounds were found mostly in the stratum corneum intercellular spaces, suggesting that although both are located within the skin barrier lipids, only the active ester is able to effectively interact with the lipids, which was proved by infrared spectroscopy of enhancer-treated *stratum corneum*. This proof-of-concept study illustrates the use of fluorescent enhancers to obtain insight into the skin penetration/permeation process; interactions among the enhancer, drug, solvent, and skin; and enhancer metabolism.


**KEYWORDS**: Transdermal drug delivery; skin; penetration enhancer; fluorescent labeling

## 1. INTRODUCTION

Skin penetration and permeation enhancers are compounds of both synthetic and natural origin that facilitate drug penetration into different skin layers (topical drug delivery) or permeation through the skin into systemic circulation (transdermal drug delivery), respectively [1]. This manner of drug administration offers many advantages over conventional application routes, *e.g.*, fewer side effects and fewer interactions with drugs and food [2]. However, the skin acts as a formidable barrier between the environment and body and effectively limits the flux of most drugs. Despite the numerous approaches to overcome the skin barrier that have been developed over recent decades (*e.g.,* chemical enhancers, ultrasound, microneedles [3]), there is still a need for new and improved strategies.

Broader use of chemical enhancers in transdermal/topical drug delivery systems is limited by their irritation potential or toxicity. Despite a wide range of compounds, mainly amphiphiles [4], showing potent penetration-enhancing effects, these effects have been drug-specific and strongly dependent on the drug's physicochemical properties [3, 5]. In addition, chemical enhancers should decrease the skin barrier properties only temporarily to prevent the access of undesirable compounds from the environment into the body or excessive water loss [1, 6]. In general, enhancers act by manipulating the skin barrier lipids, proteins or drug partitioning equilibria [7]. However, the specific mechanisms that govern the enhancer interactions with the skin and drug are not fully understood. For example, it is not known whether the drug itself somehow influences the enhancer performance during the penetration/permeation process.

Thus, the development of strategies to investigate the mechanisms involved in the interactions of enhancers with the skin (and also with other biological barriers) would significantly aid in the design of potent yet safer enhancers for transdermal and topical drug delivery. Seto *et al.*, in their pioneering study, identified naturally fluorescent enhancers (using measurements of skin current)

and visualized selected enhancers in the skin using two-photon fluorescence microscopy [8]. The most potent enhancer was Bodipy® 500/510 $C_8$, $C_5$, a compound with a boron-dipyrromethene core and two chains (octyl tail and pentanoic acid) attached to it (Figure 1). This study also described glycerol-mitigated and ultrasound-enhanced penetration enhancement [8].

In this study, we designed fluorescent penetration/permeation enhancers by combining an amphiphilic fluorophore with one of our most potent enhancers, 6-(dimethylamino)hexanoic acid dodecyl ester (DDAK; Figure 1). DDAK enhances the penetration and permeation of a broad spectrum of drugs and has limited toxicity and no dermal irritation, and its action is reversible [9-11]. In the hybrid enhancers studied here, we exchanged the dimethylamino polar head of DDAK for a fluorophore. We selected 7-nitrobenzo[c][1,2,5]oxadiazol-4-yl (NBD) instead of Bodipy® because NBD is relatively small and polar and can be easily attached to the primary amino group of an amino ester. For a review of the properties and applications of NBD-labeled lipids, see ref. [12]. We intentionally maintained the ester group in these new enhancers so that they can be hydrolyzed by esterases and their effects possibly terminated in the living epidermis.

Hence, NBD-labeled 6-aminohexanoic acid (NBD-acid) and its esters with $C_8$, $C_{10}$ and $C_{12}$ chains (NBD-C8 ester, NBD-C10 ester, and NBD-C12 ester, respectively) were prepared (Figure 1). Apart from enhancer *visualization* in the skin using confocal laser scanning microscopy, we mainly focused here on the enhancer *quantitation* during the *in vitro* penetration process in human skin in the presence of two model drugs and two model solvents. By using HPLC to separate the fluorescent enhancers, we also aimed to identify any potential degradation of the enhancers in the skin. Finally, we used confocal laser scanning microscopy to visualize the new NBD-labeled compounds, representing active and inactive enhancers, in the skin.

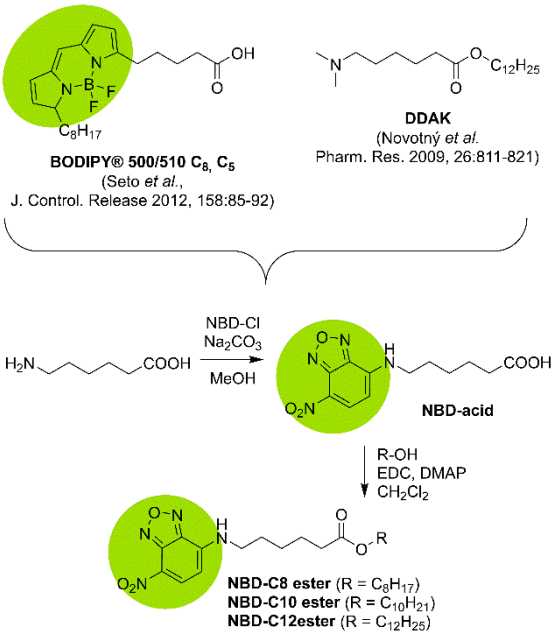


**Figure 1.** Chemical structures of the lead enhancers BODIPY® 500/510 $C_8$, $C_5$ [8] and DDAK[9] used in the design of the NBD-labeled enhancers, and their synthesis. DMAP: 4-(dimethylamino)pyridine; EDC: 1-ethyl-3-(3-dimethylaminopropyl)carbodiimide.

## 2. EXPERIMENTAL SECTION

### *2.1. Synthesis of enhancers*

Chemicals were purchased from Sigma-Aldrich (Schnelldorf, Germany) and used as received. TLC was performed on Merck aluminum plates with silica gel 60 $F_{254}$. Merck Kieselgel 60 (0.040-0.063 mm) was used for column chromatography. Melting points were recorded with a Büchi B-545 apparatus (BUCHI Labortechnik AG, Flawil, Switzerland) and are uncorrected. The structural identities of the prepared compounds were confirmed by $^{1}$H-NMR and $^{13}$C-NMR spectroscopy using a Varian Mercury VNMR S500 NMR spectrometer (Varian, Palo Alto, CA, USA) and HRMS system Acquity UPLC I-class and Synapt G2Si Q-TOF mass spectrometer (Waters, Milford, USA). Chemical shifts were reported as $\delta$ values in parts per million (ppm) and were indirectly referenced to tetramethylsilane via the solvent signal. Data are presented as follows: chemical shift, multiplicity (s = singlet, d = doublet, t = triplet, m = multiplet), coupling constant (*J*, Hz) and integration. Infrared spectra were measured using Nicolet 6700 instrument in ATR mode (Thermo Scientific, Waltham, MA, USA). Melting points were determined using a Kofler hot-stage microscope and are uncorrected. Purities of the enhancers were determined by HPLC (see below and Supporting Information).

6-((7-Nitrobenzo[c][1,2,5]oxadiazol-4-yl)amino)hexanoic acid (**NBD-acid**). 6-Aminohexanoic acid (0.23 g, 1.70 mmol) and 4-chloro-7-nitrobenzo[c][1,2,5]oxadiazole (NBD-Cl) (0.68 g, 3.40 mmol) were dissolved in MeOH, and $NaHCO_3$ (0.43 g, 5.12 mmol) in 25 mL water was added. The reaction was stirred at room temperature for 24 h; the solids dissolved in 20 min and the color changed from light orange to brown. The reaction was acidified, and the crystalline product was filtered off. The product was further purified by column chromatography on silica gel using $CHCl_3$/MeOH 50:1 (v/v) followed by $CHCl_3$/MeOH 10:1 (v/v) after the elution of unreacted NBD-Cl. Yield 35%; orange crystals, well soluble in MeOH, DMSO and $CHCl_3$, partly soluble in

water. M.p. 159-160°C (literature: 158-159°C,[13]). $R_f$ = 0.21 ($CHCl_3$/MeOH, 10:1). $^1$H NMR (500 MHz, DMSO-$d_6$): $\delta$ = 11.97 (s, 1H), 9.51 (t, $J$ = 5.9 Hz, 1H), 8.48 (d, $J$ = 9.0 Hz, 1H), 6.39 (d, $J$ = 9.1 Hz, 1H), 3.48 – 3.40 (m, 2H), 2.20 (t, $J$ = 7.3 Hz, 2H), 1.72 – 1.62 (m, 2H), 1.59 – 1.49 (m, 2H), 1.42 – 1.32 (m, 2H) ppm. $^{13}$C NMR (125 MHz, DMSO-$d_6$): $\delta$ = 174.9, 145.6, 144.9, 144.6, 138.4, 121.0, 99.6, 43.7, 34.0, 27.8, 26.4, 24.6 ppm. IR (ATR): $\nu_{max}$ 3347, 2939, 2856, 1729, 1698, 1585, 1495, 1298, 1270, 1169, 1119, 996 cm$^{-1}$. Synthesis of NBD-esters. NBD acid (50 mg, 0.17 mmol) and alcohol (octanol, decanol or dodecanol; 0.19 mmol) in anhydrous $CH_2Cl_2$ (5 mL) were cooled to 0°C under argon, and 1-ethyl-3-(3-dimethylaminopropyl)carbodiimide (EDC; 35.8 mg, 0;19 mmol) and 4-dimethylaminopyridine (DMAP; 2 mg, 0.017 mmol) in anhydrous $CH_2Cl_2$ were added. The reaction was allowed to reach room temperature and stirred under argon overnight. TLC showed incomplete conversion; thus, more EDC (9 mg, 0.05 mmol) was added and stirred for an additional 16 h. Next, the reaction was washed with 0.1 M HCl. The aqueous phase was extracted with $CHCl_3$, and the combined organic phases were evaporated and purified on silica gel using hexane/EtOAc 6:1 (v/v).

Octyl 6-((7-nitrobenzo[c][1,2,5]oxadiazol-4-yl)amino)hexanoate (**NBD-C8 ester**). Yield 47%; orange waxy substance, well soluble in MeOH, EtOAc, $CHCl_3$ and hexane. M.p. 41-42°C; $R_f$ = 0.64 ($CHCl_3$/MeOH, 20:1). $^1$H NMR (500 MHz, $CDCl_3$): $\delta$ = 8.49 (d, $J$ = 8.6 Hz, 1H, C$^6$H), 6.41 (t, $J$ = 5.8 Hz, 1H, NH), 6.18 (d, $J$ = 8.8 Hz, 1H, C$^5$H), 4.08 (t, $J$ = 6.8 Hz, 2H, O-$CH_2$), 3.57 – 3.49 (m, 2H, N-$CH_2$), 2.37 (t $J$ = 7.2 Hz, 2H, CO-$CH_2$), 1.90 – 1.80 (m, 2H, $CH_2$), 1.77 – 1.70 (m, 2H, $CH_2$), 1.66 – 1.58 (m, 2H, $CH_2$), 1.57 – 1.49 (m, 2H, $CH_2$), 1.39 – 1.19 (m, 10H, 5 $CH_2$), 0.88 (t, $J$ = 6.7 Hz, 3H, $CH_3$) ppm. $^{13}$C NMR (125 MHz, $CDCl_3$): $\delta$ = 173.5, 144.2, 143.9, 143.8, 136.4, 124.0, 98.5, 64.7, 43.7, 33.9, 31.7, 29.16, 29.14, 28.6, 28.1, 26.3, 25.9, 24.3, 22.6, 14.0 ppm. IR (ATR): $\nu_{max}$ 3318, 2926, 2856, 1721, 1596, 1497, 1324, 1270, 1178, 1130, 996 cm$^{-1}$. HRMS (TOF MS ES$^+$): $C_{20}H_{30}N_4O_5$ [M+H$^+$] Calcd.: 407.2289, found 407.2295 [M+H$^+$].

Decyl 6-((7-nitrobenzo[c][1,2,5]oxadiazol-4-yl)amino)hexanoate (**NBD-C10 ester**). Yield 56%; orange waxy substance, well soluble in MeOH, EtOAc, $CHCl_3$ and hexane. M.p. 59-62°C; $R_f$ = 0.65 ($CHCl_3$/MeOH 20:1). $^1$H NMR (500 MHz, $CDCl_3$): $\delta$ = 8.48 (d, $J$ = 8.6 Hz, 1H, C$^6$H), 6.37 (t, $J$ = 5.7 Hz, 1H, NH), 6.18 (d, $J$ = 8.6 Hz, 1H, C$^5$H), 4.07 (t, $J$ = 6.8 Hz, 2H, O-$CH_2$), 3.56 – 3.49 (m, 2H, N-$CH_2$), 2.36 (t, $J$ = 7.2 Hz, 2H, CO-$CH_2$), 1.91 – 1.81 (m, 2H, $CH_2$), 1.77 – 1.68 (m, 2H, $CH_2$), 1.65 – 1.58 (m, 2H, $CH_2$), 1.57 – 1.49 (m, 2H, $CH_2$), 1.38 – 1.19 (m, 14H, 7 $CH_2$), 0.87 (t, $J$ = 6.8 Hz, 3H, $CH_3$) ppm. $^{13}$C NMR (125 MHz, $CDCl_3$): $\delta$ = 173.5, 144.2, 143.9, 143.8, 136.4, 124.0, 98.5, 64.7, 43.7, 33.9, 31.8, 29.7, 29.5, 29.3, 29.2, 28.6, 28.1, 26.3, 25.9, 24.3, 22.6, 14.1 ppm. IR (ATR): $\nu_{max}$ 3319, 2922, 2854, 1721, 1698, 1597, 1496, 1325, 1270, 1176, 1130, 996 cm$^{-1}$. HRMS (TOF MS ES$^+$): $C_{22}H_{34}N_4O_5$ [M+H$^+$] Calcd.: 435.2602, found 435.2608 [M+H$^+$].

Dodecyl 6-((7-nitrobenzo[c][1,2,5]oxadiazol-4-yl)amino)hexanoate (**NBD-C12 ester**). Yield 39%; orange waxy substance, well soluble in MeOH, EtOAc, $CHCl_3$ and hexane. M.p. 65-67°C; $R_f$ = 0.68 ($CHCl_3$/MeOH, 20:1).$^1$H NMR (500 MHz, $CDCl_3$): $\delta$ = 8.48 (d, $J$ = 8.6 Hz, 1H, C$^6$H), 6.36 (t, $J$ = 5.8 Hz, 1H, NH), 6.17 (d, $J$ = 8.6 Hz, 1H, C$^5$H), 4.06 (t, $J$ = 6.8 Hz, 2H, O-$CH_2$), 3.55 – 3.47 (m, 2H, N-$CH_2$), 2.35 (t, $J$ = 7.3 Hz, 2H, CO-$CH_2$), 1.89 – 1.79 (m, 2H, $CH_2$), 1.76 – 1.68 (m, 2H, $CH_2$), 1.64 – 1.57 (m, 2H, $CH_2$), 1.55 – 1.48 (m, 2H, $CH_2$), 1.37 – 1.22 (m, 18H, 9 $CH_2$), 0.86 (t, $J$ = 6.8 Hz, 3H, $CH_3$) ppm. $^{13}$C NMR (125 MHz, $CDCl_3$): $\delta$ = 173.5, 144.2, 143.9, 143.8, 136.4, 124.0, 98.5, 64.7, 43.7, 33.9, 31.9, 29.67, 29.61, 29.60, 29.54, 29.50, 29.3, 29.2, 28.6, 28.1, 26.3, 25.9, 24.3, 22.7, 14.1 ppm. IR (ATR): $\nu_{max}$ 3307, 2921, 2853, 1721, 1598, 1497, 1325, 1270, 1177, 1130, 996 cm$^{-1}$. HRMS (TOF MS ES$^+$): $C_{24}H_{38}N_4O_5$ [M+H$^+$] Calcd.: 463.2915, found 463.2925 [M+H$^+$].

*2.2. Skin*

Human skin from Caucasian female patients (46-57 years) who had undergone abdominal plastic surgery was used. The procedure for this work was approved by the Ethics Committee of the University Hospital Hradec Králové, Czech Republic (No. 200609 S09P) and conducted according to the principles of the Declaration of Helsinki. The subcutaneous fat was carefully removed, and the remaining skin fragments were washed with saline, blotted dry, and stored at -20°C.

*2.3. Donor samples for penetration/permeation studies*

Donor samples were prepared as suspensions of theophylline (TH) or hydrocortisone (HC) at 5% and 2% (w/v), respectively, in propylene glycol (PG)/water(W) 6:4 (v/v) or ethanol (EtOH)/PG 7:3 (v/v) with or without the studied compounds (Table 1). All samples were allowed to equilibrate at 37°C for 24 h. The samples were resuspended before application to the skin. To determine whether the added enhancers had any effect on the solubility of the drugs in the donor solvent $C_0$ (mg/mL), that is, on their thermodynamic activity, the samples were prepared in triplicate as described above and allowed to equilibrate. After 24 h, the suspensions were centrifuged at 6,700 × g for 10 min; the supernatant was withdrawn, diluted with the phosphate-buffered saline (PBS) and analyzed by HPLC.

*2.4. Permeation/penetration experiments*

Skin permeability was evaluated using modified Franz diffusion cells with an acceptor volume of 15.7 ± 0.2 mL. The frozen human skin was slowly thawed, cut into pieces, mounted into the diffusion cells dermal side down using Teflon holders with an available diffusion area of 1 $cm^2$ and sealed with silicone grease. Full thickness skin was used because we were also interested in

the drug and enhancer concentrations in the dermis. The acceptor compartment was filled with phosphate-buffered saline (PBS, containing 10 mM phosphate buffer, 137 mM NaCl and 2.7 mM KCl) at pH 7.4 with 0.005% of gentamicin sulfate as a preservative) and stirred in a water bath at 32°C throughout the experiment. After an equilibration period of 1 h, skin integrity was checked by electrical impedance,[14] which was over 20 kΩ×cm$^2$ in all the samples (27±5 kΩ×cm$^2$). After the experiment, the impedance appeared to slightly decrease (to 81±11% of the initial impedance) but the difference was not statistically significant.

Next, 150 µL (*i.e.*, an infinite dose) of the donor sample was applied to the skin and covered with a glass slide. Sink conditions were maintained for all drugs. Samples of the acceptor phase (0.3 mL) were withdrawn at predetermined time intervals and replaced with fresh acceptor buffer solution. The amount of drug that permeated through the skin was measured by HPLC (see later). At the end of the permeation experiment (48 h for TH and 64 h for HC), the diffusion cells were dismounted, and the skin washed with PBS and a cotton swab soaked with 60% ethanol. The tissue that had been exposed to the donor sample was punched out, wrapped in aluminum foil, and heated to 80°C for 2 min in an oven. The epidermis was then carefully peeled off from the dermis. The epidermis and dermis were then weighed and extracted with 1 mL and 2 mL of acetonitrile, respectively, for 48 h. The extract was filtered and analyzed by HPLC.

Another experiment was performed with freshly excised abdominal human skin (28 years). The skin samples were placed into Teflon holders with a 1 cm$^2$ circular openings and sealed using an inert silicon grease. These assemblies were transferred into a Petri dish dermal side down onto a gauze soaked with Dulbecco´s modified Eagle´s medium (DMEM; Lonza, Verviers, Belgium). 150 µL of 1% NBD-C8 ester in PG/W was applied to the skin and incubated at 32°C. After 24 h, the skin samples were carefully rinsed by PBS and ethanol to remove residual donor sample and tape stripped using Scotch Crystal Clear tape. The first strip was discarded and the others were

pooled in the following manner: 2-3; 4-5; 6-8; 9-11; 12-16; 17-21. Then, viable epidermis was isolated from dermis by heat treatment. The tape strips, epidermis, and dermis were shaken with acetonitrile (1 mL, 1 mL, and 2 mL, respectively) at room temperature overnight, the solvent was filtered, diluted and analyzed by HPLC for NBD-C8 ester and NBD-acid.

*2.5. Stratum corneum/donor solvent partitioning coefficients*

The relative *stratum corneum*/donor solvent partitioning coefficients of the drugs and enhancers were estimated using trypsin-isolated *stratum corneum*[15] as described previously.[10] Before the experiment, *stratum corneum* sheets of ca 10 mg were precisely weighed and hydrated in 1 ml of saline with 0.005% gentamicin at 32°C. After 48 h, SC was withdrawn and blotted dry on a filter paper. Donor solution ($c_0$) containing 10 µg/ml drug, either with or without the NBD esters (10 µg/ml), in PG/W or EtOH/PG was added to each *stratum corneum* sheet at 1 ml/10 mg. The samples were equilibrated at 32°C for 24 h, centrifuged at 6.700 × g for 5 min, and the concentrations of the drugs and enhancers in the supernatant were determined by HPLC ($c_{donor}$). The partitioning coefficient $P$ was determined as follows: $P = (c_0 - c_{donor})/c_{donor}$.

*2.6. High-performance liquid chromatography (HPLC)*

The model drugs and enhancers were determined by reverse-phase HPLC using a Shimadzu Prominence instrument (Shimadzu, Kyoto, Japan) consisting of LC-20AD pumps with a DGU-20A3 degasser, a SIL-20A HT autosampler, a CTO-20AC column oven, an SPD-M20A diode array detector, an RF10AXL fluorescence detector, and a CBM-20A communication module. Data were analyzed using the LCsolutions 1.22 software. Model drugs and enhancers were analyzed on a LiChroCART 125-4 column (Purospher STAR RP-8e, 5 µm, Merck, Darmstadt, Germany) at 30°C using 0.5% aqueous acetic acid/acetonitrile mobile phase at a flow rate of 1.5

mL/min. The effluent was measured at 270 nm for TH, 244 nm for HC and at 466/539 nm (excitation/emission) for enhancers. For the simultaneous analysis of TH and enhancers, the concentration of acetonitrile was initially 10% (0 – 1.5 min), followed by a linear gradient from 10 to 90% (1.5 - 2.5 min), 90% (2.5 - 6.5 min) and 10% (6.6 - 11.5 min). Retention times were as follows: 1.9 min (TH), 4.9 min (NBD-acid), 5.9 min (NBD-C8 ester), 6.2 min (NBD-C10 ester) and 6.5 min (NBD-C12 ester). For the simultaneous analysis of HC and enhancers, the concentration of acetonitrile was 40% (0 – 2.3 min), then a linear gradient from 40 to 90% (2.3 - 2.5 min), 90% (2.5 - 6.8 min) and 40% (6.9 - 11.5 min). Retention times were as follows: 1.5 min (HC), 2.1 min (NBD-acid), 5.9 min (NBD-C8 ester), 6.2 min (NBD-C10 ester) and 6.5 min (NBD-C12 ester). The precision and accuracy of these methods were within the limits of the FDA guidelines for bioanalytical method validation (2001). The calibration curves were linear over the range 0.5 – 100 μg/mL for TH and HC, and 0.005 – 100 ng/mL for the enhancers ($r^2 \geq 0.999$, $p < 0.001$).

*2.7. Confocal laser scanning microscopy*

The localization of NBD-C8 ester and NBD-acid in the human epidermis was imaged using confocal laser scanning microscopy. Donor samples were prepared as 0.1% suspensions of the enhancer in PG/W 6:4 (v/v) and allowed to equilibrate at 32°C for 12 h. Freshly excised human skin was separated from the subcutaneous fat, dermatomed to 500 μm, and cut to samples of approximately 4 $cm^2$ areas. These skin samples were placed into a Petri dish onto a cotton gauze soaked with 0.4% solution of dispase II (protease from *Bacillus polymyxa*; ≥ 0.5U/mg; Sigma-Aldrich, Schnelldorf, Germany) in PBS. After the incubation at 37°C for 1 h, the epidermis was gently peeled off the dermis. The epidermal sheets were transferred into Teflon holders with a 2 $cm^2$ circular opening sealed using an inert silicon grease. The holders with epidermal sheets were

placed into a Petri dish basal side down onto a cotton gauze soaked with DMEM. The donor sample of 200 µl was applied on the epidermis. After 24 h at 32°C, the skin samples were carefully rinsed by PBS and ethanol to remove residual donor sample, transferred into a Petri dish with Hoechst 33342 (Molecular Probes, Eugene, OR, USA) in PBS (0.03 mg/mL), and stained at 32°C for 20 min. Subsequently, the epidermal samples were rinsed with water and PBS, transferred on a clean glass slide and the images were taken using Nikon A1+ confocal microscope (Nikon, Tokyo, Japan). For each sample, 15 focal planes (step 3.0 µm) were taken using 405 nm and 488 nm lasers with the respective emission filters (DAPI, FITC). The pinhole was set up at 17.9 µm, and laser power was kept as low as possible to prevent any photodamage to the sample.

*2.8. Fourier transform infrared (FTIR) spectroscopy*

Epidermis was isolated by heating the human skin to 60°C for 2 min. The *stratum corneum* sheets were isolated by trypsin treatment [16]. Before the experiment, hydrated *stratum corneum* sheets were cut into small pieces and treated with 10 µL of PG/W (control), 1% NBD-acid or 1% NBD-C8 ester in PG/W at 32°C. After 24 h, the excess donor sample was carefully removed, and the samples were examined by FTIR. Spectra of the samples were collected on a Nicolet 6700 FT-IR spectrometer (Thermo Scientific, USA) equipped with a single-reflection MIRacle attenuated total reflectance ZnSe crystal. A clamping mechanism with a constant clamping pressure was used for all experiments. The spectra were generated by co-addition of 128 scans collected at a resolution of 2 $cm^{-1}$. The spectra were analyzed using the Bruker OPUS software.

*2.9. Data treatment*

The cumulative amount of the drug permeated across the skin, corrected for the acceptor phase replacement, was plotted against time, and the steady-state flux $J_{SS}$ (μg/cm$^2$/h) was calculated from the linear region of the plot. The flux were also calculated using the free SAMPA software [17]; no significant differences in flux between these two methods were found. The enhancement ratio (ER) was calculated as a ratio of the drug flux with and without the enhancer. The permeability coefficient *Kp* (cm/h) was calculated by dividing $J_{SS}$ by the donor concentration of the model drug $C_0$ (mg/mL) or enhancer $C_E$ (mg/mL). The concentration of the model drugs and enhancers in epidermis and dermis were calculated by dividing the amount of the drug/enhancer by the respective tissue weight. The statistical analysis was performed with the GraphPad Prism statistical program (version 6.07; GraphPad Software, La Jolla, CA, USA). For the comparison of two groups, Student's t-test was used, and for the comparison of three or more groups, a one-way ANOVA test with Dunnett's multiple comparisons post hoc test was used. The differences between results were considered significant at $p < 0.05$. Data are presented as the means ± SEM, and the number of replicates (*n*) is given in the pertinent figures.

## 3. RESULTS AND DISCUSSION

### *3.1. Synthesis and properties of NBD esters*

First, NBD-acid was prepared from aminohexanoic acid using a modified procedure described previously [13, 18]. Although crystallization was described to yield a product of sufficient purity, we had to employ additional chromatography to remove 6-aminohexanoic acid residue. The reaction yields were the same with aqueous $Na_2CO_3$ [18] or under anhydrous conditions [13]. The final esters were then prepared via carbodiimide coupling of the NBD-acid and pertinent alcohols with 8, 10, and 12 carbons.

The NBD esters were waxy orange compounds, strongly fluorescent in solutions, with melting points 41-67°C. The predicted logP values (or, more precisely fragment/compound ClogP calculated using ChemBioDraw) of NBD esters were 6.9-9. The lipophilicity of NBD-C8 ester was very close to the lead fluorescent enhancer, Bodipy® 500/510 $C_8$, $C_5$ [8] (Clog P 7.2). In contrast to esters, the NBD-acid had a ClogP of 2.8 and was slightly soluble in water.

### *3.2. Effects of NBD enhancers on the flux of model drugs TH and HC through the skin*

The penetration/permeation enhancing properties of the NBD esters in comparison to the parent NBD-acid were studied using human skin and two model drugs, TH and HC (Table 1). These two drugs were selected solely as model compounds of different size and polarity for this proof-of-concept study with no intention of transdermal/topical therapeutic application. The donor solvents, PG/W 6:4 and EtOH/PG 7:3, were previously used in numerous transdermal/topical studies [9, 11, 13, 19-22]. These two different solvent systems (PG/W 6:4 as a relatively inert solvent to skin lipids, EtOH/PG 7:3 as a system that acts via various mechanisms including lipid extraction [6]) were selected on purpose the probe the behavior of the enhancers in such different environments and to unravel possible synergies.

**Table 1.** The composition of the donor samples for penetration/permeation studies, properties of the model drugs (molecular weight, MW, and lipophilicity, logP) and the solubilities of model drugs and enhancers in the donor samples

| Model drug | MW (g/mol) | logP | Donor solvent | Enhancer | Drug solubility $C_0$ (mg/mL) | Enhancer solubility $C_E$ (mg/mL) |
|---|---|---|---|---|---|---|
| Theophylline (TH) | 180.2 | -0.02 | propylene glycol/ water (PG/W) 6:4 (v/v) | - | 25.8 ± 1.1 | - |
| | | | | NBD-acid | 25.7 ± 1.0 | 2.20 ± 0.12 |
| | | | | NBD-C8 ester | 25.4 ± 0.7 | 0.12 ± 0.03 |
| | | | | NBD-C10 ester | 24.1 ± 0.7 | 0.07 ± 0.02 |
| | | | | NBD-C12 ester | 24.5 ± 0.4 | 0.01 ± 0.003 |
| | | | ethanol/ propylene glycol (EtOH/PG) 7:3 (v/v) | - | 10.9 ± 0.6 | - |
| | | | | NBD-acid | 11.7 ± 0.6 | 8.97 ± 0.41 |
| | | | | NBD-C8 ester | 11.9 ± 0.5 | 8.77 ± 0.34 |
| | | | | NBD-C10 ester | 11.1 ± 0.2 | 8.50 ± 0.17 |
| | | | | NBD-C12 ester | 10.2 ± 0.4 | 3.00 ± 0.12 |
| Hydrocortisone (HC) | 362.5 | 1.61 | PG/W 6:4 (v/v) | - | 6.6 ± 0.1 | - |
| | | | | NBD-acid | 6.4 ± 0.3 | 1.29 ± 0.13 |
| | | | | NBD-C8 ester | 7.1 ± 0.1 | 0.10 ± 0.04 |
| | | | | NBD-C10 ester | 6.3 ± 0.5 | 0.10 ± 0.02 |
| | | | | NBD-C12 ester | 5.8 ± 0.3 | 0.11 ± 0.03 |
| | | | EtOH/PG 7:3 (v/v) | - | 16.1 ± 0.7 | - |
| | | | | NBD-acid | 19.4 ± 0.4 | 7.90 ± 0.86 |
| | | | | NBD-C8 ester | 16.9 ± 0.4 | 8.87 ± 0.15 |
| | | | | NBD-C10 ester | 16.3 ± 0.8 | 10.50 ± 0.55 |
| | | | | NBD-C12 ester | 17.8 ± 3.0 | 4.40 ± 0.50 |

The TH solubilities in PG/W 6:4 were approximately 26 mg/mL and decreased to approximately 11 mg/mL in the more lipophilic solvent mixture, EtOH/PG 7:3 (Table 1). The solubilities of the larger and more lipophilic HC were approximately 7 mg/mL in PG/W 6:4 and 16 mg/mL in EtOH/PG 7:3. Thus, all drug samples were applied to the skin at their maximum thermodynamic activity. The drug solubilities were not significantly affected by their co-application with the NBD enhancers. In addition, the solubilities of TH and HC in the acceptor buffer were 7.65 ± 0.02 mg/ml and 0.28 ± 0.01 mg/ml, respectively, which were adequate to maintain sink conditions throughout the experiments.

The solubilities of the NBD esters in the donor media were 0.01-0.12 mg/mL in PG/W 6:4 and 3-10.5 mg/mL in the more lipophilic EtOH/PG 7:3. The solubility of NBD-acid was 1-2 mg/mL in PG/W 6:4 and 8-9 mg/mL in EtOH/PG 7:3 (Table 1). No decomposition of the esters or drugs was found in donor or acceptor media.

The flux of TH from PG/W 6:4 without enhancers was 0.8 ± 0.2 μg/cm$^2$/h (Figure 2A and Table 2). The NBD-acid had no significant effect on the skin permeability to TH, whereas the esters increased the flux values to 1.9-3.1 μg/cm$^2$/h. The greatest effect was observed in NBD-C12 ester (enhancement ratio, ER, was 3.9), followed by NBD-C8 ester (ER 3.3). The lag times were 11-17 h. For HC as the model drug, the lag time was approximately 25 h; thus, the experiment was prolonged to 64 h (Figure 2B and Table 2). The control flux from PG/W 6:4 (0.03 ± 0.01 μg/cm$^2$/h) was two orders of magnitude lower than for TH, which corresponds to the differences in their physicochemical properties. NBD esters increased the flux of HC to 0.12-0.20 μg/cm$^2$/h (ER values 3.9-6.6) with the maximum at NBD-C10 ester; NBD-acid was inactive.

A more lipophilic donor solvent, EtOH/PG 7:3, resulted in approximately 6-12 times higher flux values of TH (5.0 ± 0.7 μg/cm$^2$/h) and HC (0.36 ± 0.09 μg/cm$^2$/h) compared to PG/W 6:4 (Figures 2E and F, respectively, and Table 2). This cannot be explained by the change in solubilities of these drugs in these solvents because the solubility of HC increased by only approximately twice in EtOH/PG 7:3 compared to PG/W 6:4, and the solubility of TH actually decreased by half. The permeability coefficient *Kp*, which is independent of the donor concentrations of the drugs, increased 14.8 and 4.4 times for TH and HC, respectively, upon the change of donor solvent from PG/W 6:4 to EtOH/PG 7:3. Thus, the change in the donor solvent increased the skin permeability of both model drugs. The effects of the enhancers were, however, less pronounced in the EtOH/PG 7:3 donor solvent; with ER up to 2 for TH (with NBD-C8 ester) and up to 3 for HC (with NBD-C10 ester). Upon the solvent change from PG/W 6:4 to EtOH/PG

7:3 the $K_p$ values for TH increased 7.5, 8.1, 9.4, and 5.5 times in the presence of NBD-acid, NBD-C8, NBD-C10, and NBD-C12 esters, respectively, whereas the $K_p$ values for HC increased only 2.8, 2.2, 2.2, and 2.4 times, respectively. In fact, the permeation profiles of TH and HC from EtOH/PG solvent show long lag times (or apparent biphasic permeation - Figures 2E and F). This can be explained by that the permeation of EtOH into *stratum corneum* can alter the solubility properties of the tissue with a consequent improvement for drug partitioning into the membrane. It is also feasible that the rapid permeation of EtOH, or evaporative loss of this volatile solvent, from the donor phase modifies the thermodynamic activity of the drug within the formulation, or that EtOH extracts some *stratum corneum* lipids [6].

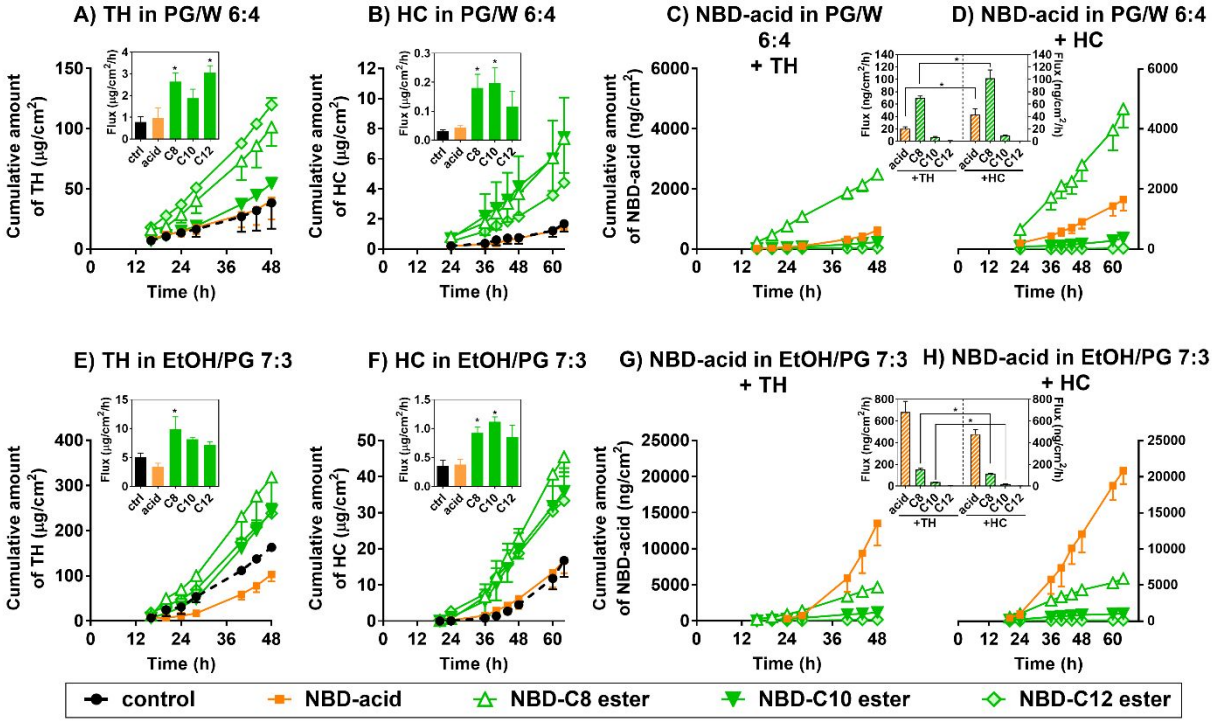


**Figure 2.** Permeation profiles of TH (panels A and E), HC (panels B and F) and NBD-acid (panels C, D, G, and H) and the corresponding flux values (inserts). The upper row (panels A – D) shows permeation from PG/W 6:4 donor samples and the lower row (panels E – H) from EtOH/PG 7:3 donor samples. Panels C and G show permeation of NBD-acid from samples of NBD-acid or the NBD esters co-applied with TH; Panels D and H show permeation of NBD-acid from samples of NBD-acid or the NBD esters co-applied with HC. Data are shown as the means

± SEM ($n$ = 3-4) and * indicates a statistically significant difference compared to the respective control or as indicated at $p < 0.05$.

**Table 2.** Permeability characteristics of the drugs and enhancers: flux ($J$) values for TH, HC and NBD-acid (the NBD esters were not detected in the acceptor solvent), the corresponding permeability coefficients ($Kp$) and enhancement ratios ($ER$).

| Drug | Donor solvent | Enhancer | Drugs (TH or HC) | | | NBD-acid | |
|---|---|---|---|---|---|---|---|
| | | | $J$ (μg/cm²/h) | $ER$ | $Kp$ ($10^{-6}$ cm/h) | $J$ (ng/cm²/h) | $Kp$ ($10^{-6}$ cm/h) |
| TH | PG/W 6:4 (v/v) | - | 0.8 ± 0.2 | - | 31 | - | - |
| | | NBD-acid | 1.0 ± 0.5 | 1.3 | 39 | 20 ± 3 | 9 |
| | | NBD-C8 ester | 2.6 ± 0.4* | 3.3 | 102 | 70 ± 3 | 807 |
| | | NBD-C10 ester | 1.9 ± 0.4 | 2.4 | 79 | 7 ± 1 | 148 |
| | | NBD-C12 ester | 3.1 ± 0.3* | 3.9 | 127 | 1.0 ± 0.1 | 157 |
| | EtOH/PG 7:3 (v/v) | - | 5.0 ± 0.7 | - | 459 | - | - |
| | | NBD-acid | 3.4 ± 0.6 | 0.7 | 291 | 680 ± 99 | 76 |
| | | NBD-C8 ester | 9.9 ± 2.1* | 2.0 | 831 | 152 ± 12 | 24 |
| | | NBD-C10 ester | 8.2 ± 0.3 | 1.6 | 739 | 36 ± 2 | 6 |
| | | NBD-C12 ester | 7.2 ± 0.5 | 1.4 | 706 | 6 ± 1 | 3 |
| HC | PG/W 6:4 (v/v) | - | 0.03 ± 0.01 | - | 5 | - | - |
| | | NBD-acid | 0.04 ± 0.01 | 1.4 | 7 | 43 ± 9 | 33 |
| | | NBD-C8 ester | 0.18 ± 0.04* | 6.0 | 25 | 102 ± 13 | 1412 |
| | | NBD-C10 ester | 0.20 ± 0.05* | 6.6 | 31 | 9 ± 1 | 133 |
| | | NBD-C12 ester | 0.12 ± 0.05 | 3.9 | 20 | 0.6 ± 0.1 | 8 |
| | EtOH/PG 7:3 (v/v) | - | 0.36 ± 0.09 | - | 22 | - | - |
| | | NBD-acid | 0.38 ± 0.09 | 1.0 | 20 | 479 ± 41 | 60 |
| | | NBD-C8 ester | 0.92 ± 0.10* | 2.6 | 54 | 113 ± 4 | 18 |
| | | NBD-C10 ester | 1.12 ± 0.09* | 3.1 | 68 | 20 ± 1 | 3 |
| | | NBD-C12 ester | 0.85 ± 0.20 | 2.4 | 48 | 2.5 ± 0.5 | 1 |

These results demonstrate that the fluorescent tag does not prevent these amphiphiles from acting as permeation enhancers. The ERs up to 6.6 are approximately comparable to the effects of the best fluorescent enhancers identified previously; the skin current ERs of the most potent fluorophores (led by Bodipy® 500/510 $C_8$, $C_5$) were approximately 2 compared to neat solvent (40% EtOH) [8]. Both enhancers in this and the previous study were applied to the skin at a 1%

concentration. Compared to DDAK, the NBD esters are weaker enhancers; because the ERs of DDAK for TH, HC, adefovir, and indomethacin were 17, 43, 14 and 9, respectively [9]. However, these fluorescent enhancers are not intended for clinical use and any extrapolation of our findings to other enhancers including the parent DDAK should be cautious because the fluorescent tag alters the physicochemical properties of the enhancer. One difference in the chemical structures of DDAK and NBD-C12 ester that may contribute to their difference in skin permeation/penetration enhancer activities is the diminished basicity of the nitrogen connected do the NBD ring. Thus, the NBD esters are not protonated at physiological pH. Additionally, in the non-ionized form, the nitrogens are different: in DDAK, the tertiary amine only acts as a hydrogen bond acceptor, while in NBD esters, the secondary nitrogen acts as a hydrogen bond donor and acceptor. The hydrogen bonds were previously found to influence the enhancer´s action [19, 23]. The second difference is the NBD ring itself. Although the cycle is polar enough to behave as a polar head of the amphiphile (when attached to the acyl chain of phospholipid it even loops up to the polar region of the membrane as shown by fluorescence quenching studies, reviewed in Chattopadhyay [12]), it is much bulkier than the dimethylamino group in DDAK. Despite these differences, the advantage of the NBD-labeled enhancers is that they can easily be visualized/quantified in the skin to gain deeper insight into the enhancer behavior during the penetration process.

*3.3. Permeation of NBD enhancers through the skin*

Apart from determining the effects of NBD enhancers on the flux of model drugs, we aimed to simultaneously quantify the flux of the NBD esters themselves and their precursor (or putative hydrolysis product), NBD-acid. Thus, we analyzed the acceptor samples for these enhancers. Despite the low quantification limits for these highly fluorescent compounds (pg/mL), no NBD

esters were found in the acceptor media. This was expected given the high lipophilicities of such compounds [13]. However, all acceptor samples under the skin that received NBD esters contained NBD-acid (Figures 2C, D, G and H and Table 2). Because all NBD esters were stable in both the donor and acceptor solvents, this finding suggests enzymatic hydrolysis by skin esterases [24] despite the skin used being frozen/thawed.

Using PG/W 6:4 donor sample with TH as a model drug, the flux of NBD-acid was higher with NBD-C8 ester (70 ± 3 ng/cm$^2$/h) than from the sample with NBD-acid (20 ± 3 ng/cm$^2$/h) (Figure 2C and Table 2). With a further increase in lipophilicity of the NBD esters, the flux values of NBD-acid dramatically decreased. To account for the differences in the donor solubility and MW of the NBD derivatives, *Kp* values were calculated ($Kp = J/C_0 * MW_{ester}/MW_{acid}$; Table 2). The *Kp* values suggest that all NBD esters actually penetrate the highly lipophilic *stratum corneum* better than NBD acid, but then the esters are partly hydrolyzed, and only the acid is able to penetrate deeper to the skin or partition into the aqueous acceptor buffer. Interestingly, with the more lipophilic HC as a model drug, both flux and *Kp* values of the NBD-acid (applied as NBD-acid or NBD-C8 ester) were approximately two times *higher* than those with TH (Figure 2D and Table 2).

When we changed the donor sample to EtOH/PG 7:3, NBD-acid gave the highest flux values, followed by the esters according to their lipophilicity (Figures 2G-H and Table 2). In this solvent, HC compared to TH significantly *decreased* the permeation of NBD-acid from the samples with NBD-C8 ester and NBD-C10 ester. Notably, upon the solvent change from PG/W 6:4 to EtOH/PG 7:3, the $K_p$ values of the NBD-acid (when applied as NBD-acid) increased 8.4 and 1.8 times when co-applied with TH and HC, respectively. Thus, the drug also modified the solvent effect. In contrast, when the NBD-C8, NBD-C10, and NBD-C12 esters were applied, the donor

solvent shift actually decreased the NBD-acid permeabilities 34, 25 and 52 times, respectively (when co-applied with TH) and 78, 44 and 8 times, respectively (when co-applied with HC). These results demonstrate that not only enhancers influenced the permeation of the drug, which is expected from an enhancer, but also the drug changed the permeation of the enhancers. These drug effects on the flux of enhancers were either positive or negative depending on the solvent used, which points to rather complex interactions among the drug, enhancer, solvent, and the skin. Because the general mechanisms of the penetration/permeation enhancement include interactions with the *stratum corneum* lipids, proteins or alteration of the compound partitioning equilibria [6, 7], the drugs likely changed some of these parameters.

*3.4. Stratum corneum/donor solvent partitioning coefficients of TH, HC, and NBD esters*

The relative partitioning coefficients *P* of the drugs and NBD esters between the *stratum corneum* and donor solvents are shown in Figure 3. Using PG/W 6:4 donor solvent, *P* of TH was 0.04 ± 0.01 and it was not affected by any of the esters. With the EtOH/PG 7:3 donor solvent, *P* of TH increased 5 times to 0.23 ± 0.06. This greater partitioning into the tissue from EtOH/PG compared to PG/W is consistent with the lower TH solubility in this solvent (hence greater escaping tendency of the drug). The NBD-C8 ester significantly decreased TH partitioning into the *stratum corneum.* With longer-chain esters, the *P* values gradually increased up to that of control without enhancers. The *P* values of HC without enhancers were 0.26 ± 0.05 and 0.08 ± 0.01 from PG/W 6:4 and EtOH/PG 7:3, respectively. The higher partitioning into the *stratum corneum* from PG/W than from EtOH/PG is consistent with the lower solubility of this lipophilic drug in this donor solvent. The enhancers either had no effect or decreased the *P* values of HC (Figures 3B and 3E). Thus, the enhancing potencies of the NBD esters for TH and HC do not involve increased drug partitioning.

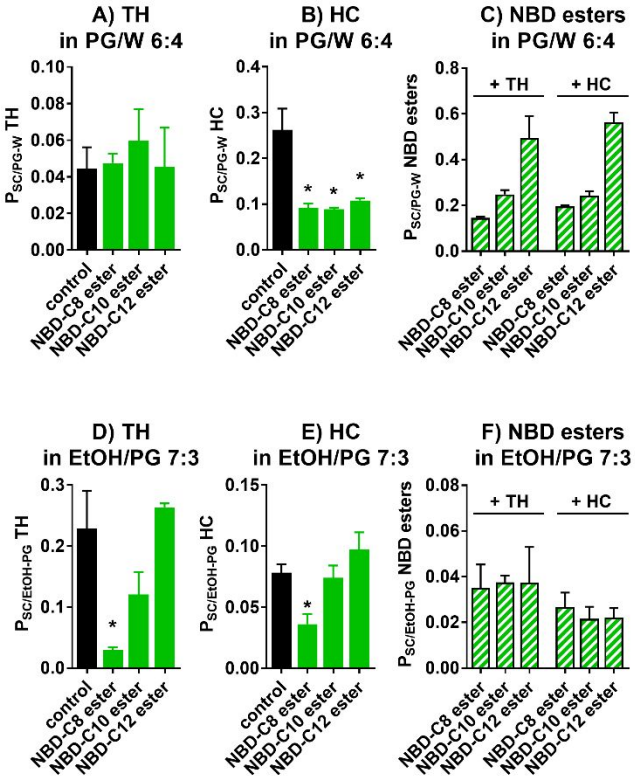


**Figure 3.** Relative *stratum corneum*/donor partitioning coefficients (*P*) of TH (panels A and D), HC (panels B and E), and NBD esters co-applied with TH or HC (panels C and F). The upper row (panels A – C) shows the data using PG/W 6:4 donor samples and the lower row (panels D – F) using EtOH/PG 7:3 donor samples. Data are shown as the means ± SEM ($n = 4$) and * indicates statistically significant difference compared to the respective control at $p < 0.05$.

Simultaneously, we determined the *P* values of the NBD esters (Figures 3C and 3F). In PG/W 6:4, the *P* values increased with longer enhancer chain (0.15 – 0.56) with no significant influence of the drug. Using EtOH/PG 7:3 as a donor solvent resulted in lower *P* values (0.02 – 0.04) compared to those in PG/W, which are consistent with the grater solubility of the lipophilic NBD esters in this solvent. HC appeared to slightly decrease the *P* values of the esters compared to TH, but the differences were not significant. Thus, the differences in the TH and HC effects on the

enhancer permeabilities cannot be explained by their different partitioning into the *stratum corneum*.

*3.5. Effects of NBD enhancers on the retention of model drugs TH and HC in epidermis and dermis*

To probe the behavior of these drug-enhancer-solvent combinations further, we analyzed their concentrations in the epidermis and dermis (Figures 4 and 5, respectively). The TH concentrations in the epidermis reached 2.8 ± 0.4 μg/mg and 5.9 ± 1.1 μg/mg from PG/W 6:4 and EtOH/PG 7:3, respectively. In the dermis, the TH concentrations were 0.11 ± 0.02 μg/mg and 0.43 ± 0.08 μg/mg from PG/W 6:4 and EtOH/PG 7:3, respectively. The higher values from EtOH/PG 7:3 correspond to the higher flux of TH from this solvent. The concentrations of HC reached 18.6 ± 2.7 μg/mg and 16.6 ± 8.2 μg/mg in the epidermis from PG/W 6:4 and EtOH/PG 7:3, respectively, and 10.5 ± 2.0 μg/mg and 8.3 ± 2.2 μg/mg in the dermis from these solvents. Neither TH nor HC retention in either skin layer was significantly affected by the studied enhancers. Thus, the enhancers increased transdermal permeation but not delivery of these two model drugs into the epidermis/dermis.

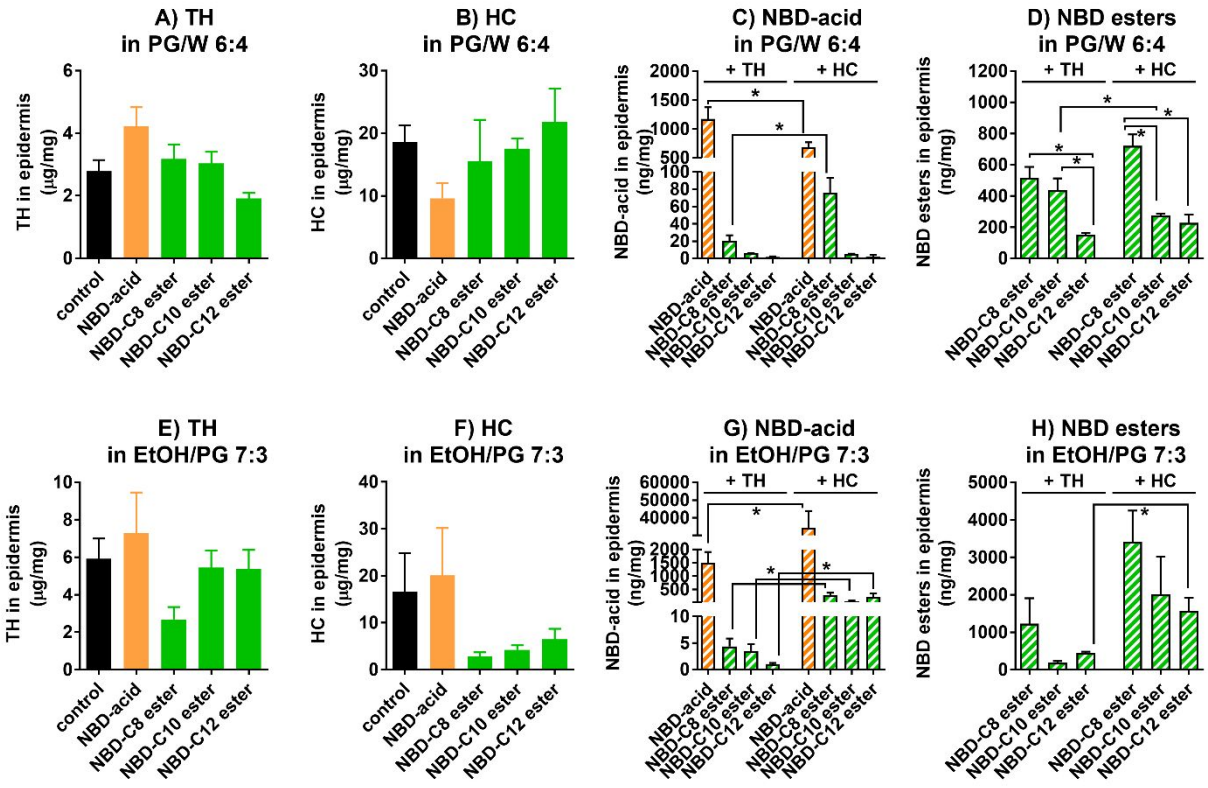


**Figure 4.** Epidermal concentrations of TH (panels A and E), HC (panels B and F), NBD-acid (from samples of NBD-acid or the NBD esters co-applied with TH or HC; panels C and G) and intact NBD esters co-applied with TH or HC (panels D and H). The upper row (panels A – D) shows permeation from PG/W 6:4 donor samples and the lower row (panels E – H) from EtOH/PG 7:3 donor samples. Data are shown as the means ± SEM ($n$ = 3-4) and * indicates statistically significant difference as indicated at $p < 0.05$.

*3.6. Concentrations of intact NBD esters and NBD-acid in the epidermis and dermis*

The analysis of the enhancers in the epidermis after the applications of the NBD esters revealed both NBD-acid and intact esters (Figures 4C-D and G-H). In the epidermis, the concentrations of the esters decreased from NBD-C8 ester to NBD-C12 ester, that is, with their increasing lipophilicity, while no such trends were observed in the dermis. Differences in enhancer concentrations were found when applied with TH or HC; however, we cannot attribute these differences solely to the effect of the drug (in contrast to flux) because the experiments with HC were run for a longer time (64 h compared to 48 h for TH). Despite the longer application time,

the concentrations of NBD-acid were actually slightly *lower* when co-applied with HC than with TH in PG/W 6:4 (except for the application of NBD-C8 ester).

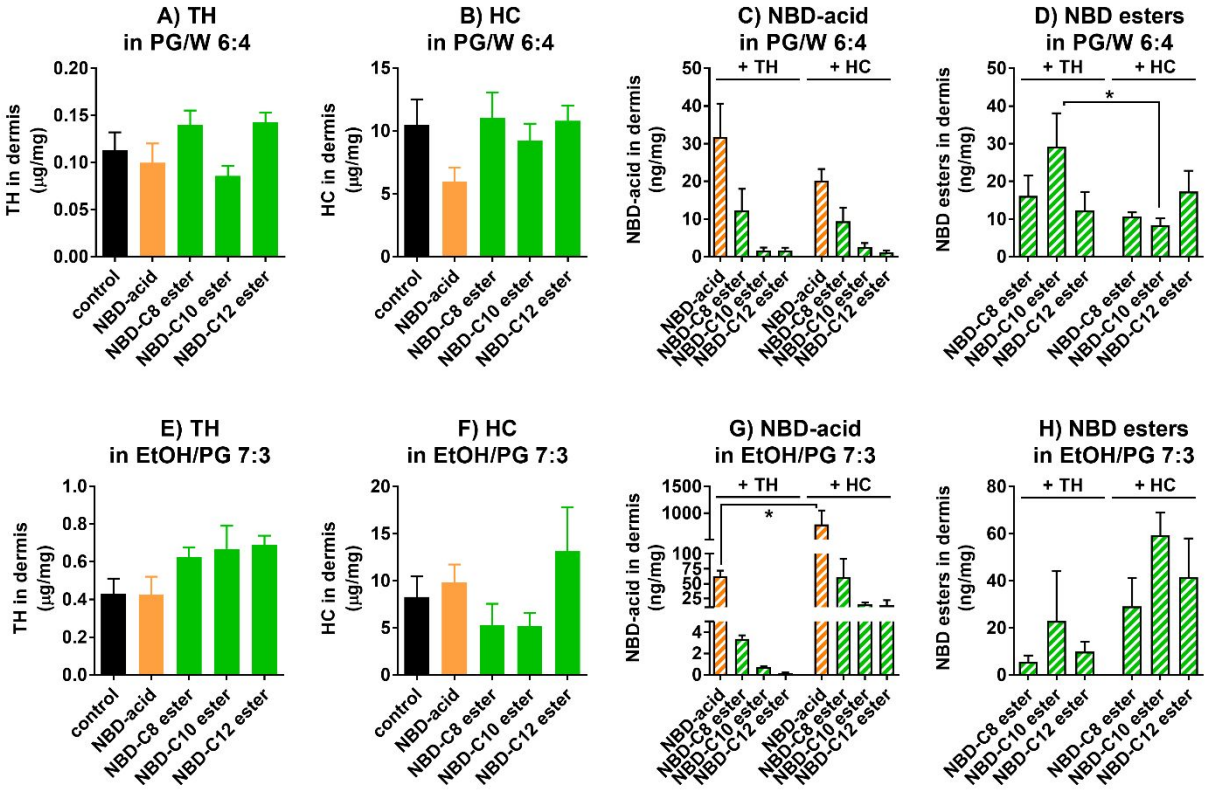


**Figure 5.** Dermal concentrations of TH (panels A and E), HC (panels B and F), NBD-acid (from samples of NBD-acid or the NBD esters co-applied with TH or HC; panels C and G) and intact NBD esters co-applied with TH or HC (panels D and H). The upper row (panels A – D) shows permeation from PG/W 6:4 donor samples and the lower row (panels E – H) from EtOH/PG 7:3 donor samples. Data are shown as the means ± SEM ($n$ = 3-4) and * indicates statistically significant difference as indicated at $p < 0.05$.

The NBD-acid comprised approximately 6 molar % of the NBD-labeled compounds in the epidermis. Thus, the hydrolysis of esters occurred in this layer but was not complete, and significant amounts of esters remained. In the dermis, both NBD-acid and NBD esters were detectable in an approximate 1:2.5 molar ratio (Figures 5C-D and G-H). This indicates that the hydrolyzed NBD-acid penetrated into the deeper, more hydrophilic skin layers faster than the parent NBD-esters. The total absorbed amounts of NBD esters and acid give the percentages of

hydrolyzed NBD-C8 ester, NBD-C10 ester and NBD-C12 ester of approximately 26, 12 and 5%. Thus, the longer the chain, the less hydrolyzed it is.

To probe the enhancer metabolism further, we performed an additional experiment using freshly excised human skin treated with NBD-C8 ester for 24 h. The tape stripping of the *stratum corneum* revealed that the amounts of ester decreased with the *stratum corneum* depth (from 3.6 nmol in pooled strips 2-3 to 1.7 nmol in pooled strips 16-21) (Figure 6). In fact, most NBD-C8 ester was retained in the *stratum corneum* (93%), whereas the viable epidermis and dermis only contained 4 and 3%, respectively, of the total amount of this compound detected in the skin. In contrast, the amount of the released NBD-acid increased with the skin depth. In the viable epidermis and dermis, the NBD-acid comprised 5 and 54 molar %, respectively, of the NBD-labeled compounds. The ester hydrolysis into NBD-acid occurred already in the lower *stratum corneum* layers (up to 3 molar % conversion). These findings are consistent with previous studies that found esterase activities in the *stratum corneum* of human volunteers by tape stripping[25] or in porcine *stratum corneum* under various experimental conditions [26].

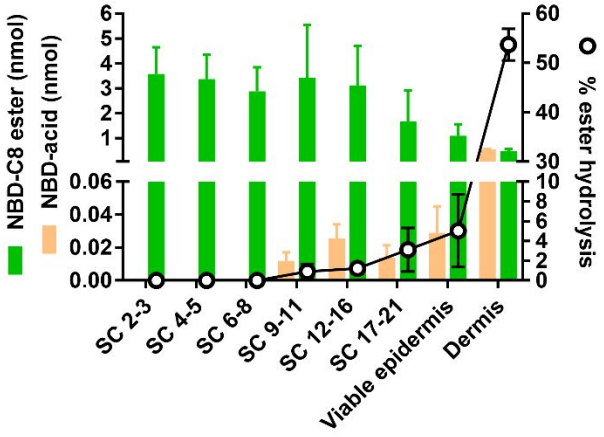


**Figure 6.** Penetration of NBD-C8 ester (green bars) and its hydrolysis into NBD-acid (yellow bars) in freshly excised human skin.

Although some properties of NBD-labeled compounds may change significantly (*e.g.,* domain formation in lipid membranes [27]), Pagano and Sleight suggested that the metabolism and intracellular translocation of NBD-labeled lipids reflected the behavior of endogenous lipids quite well [28]. However, DDAK was rapidly metabolized by porcine esterase, with a half-life of 17 min [9], whereas the metabolism of the NBD esters found here was much slower. One possible reason for this difference is that the metabolic activity in the skin is much lower than that in the liver [24]. However, the behavior of the NBD esters in the skin illustrates well the principle of the design of biodegradable enhancers.

*3.7. Visualization of NBD-labeled enhancers in the epidermis*

The fluorescent penetration/permeation enhancers were previously directly visualized in the skin by two-photon fluorescence microscopy. In the absence of ultrasound, the fluorescent enhancer remained localized in the *stratum corneum* intercellular spaces, that is, within the barrier lipids [8]. To complement our quantitative data with a visualization of a selected enhancer in the skin, we employed confocal laser scanning microscopy, a method used to study the mechanisms of diverse skin absorption enhancement strategies [29], time dependence of the enhancement effects [30] or the effects of lipophilicity and vehicle on the accumulation of dyes in human skin follicles [31].

The confocal laser scanning microscopy images of NBD-acid- and NBD-C8 ester-treated fresh skin samples are shown in Figure 7. In the NBD-acid-treated skin, NBD-acid apparently remained localized mainly within the intercellular spaces of the *stratum corneum* or, more precisely, its concentration in the intercellular region was much higher than that in the cells. No fluorescence was found in the living epidermis (with cell nuclei stained with Hoechst 33342 dye). A similar scenario was found for a selected ester, NBD-C8 ester: this compound remained in the *stratum corneum*, mostly within the lipid matrix surrounding the corneocytes, with some

fluorescence found in the corneocytes. Using this setup, no endogenous skin fluorescence was detected (Supporting Information).

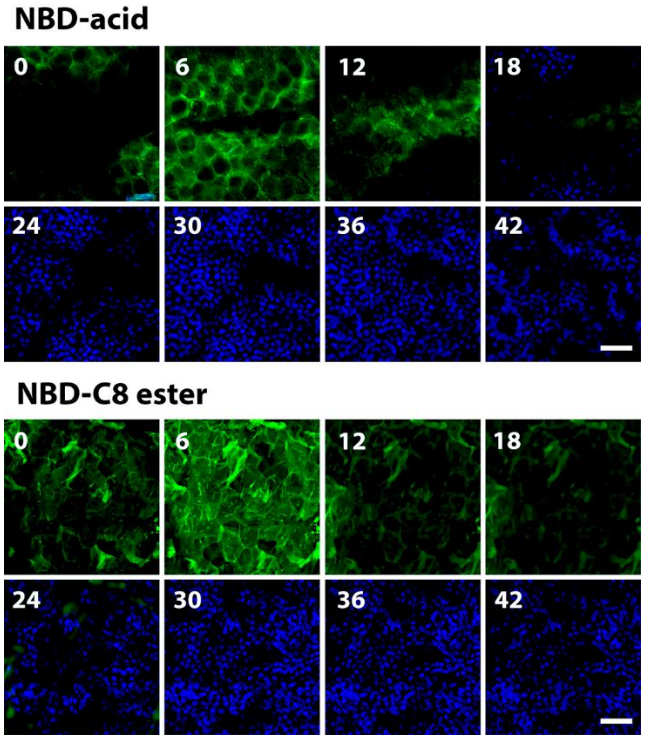


**Figure 7.** Confocal laser scanning microscopy images of NBD-acid- and NBD-C8 ester-treated skin samples. Green - intrinsic fluorescence of enhancers; blue – Hoechst 33342. Numbers represent distance (μm) in z-axis from the first focal plane (depth in the sample). Each bar represents 100 μm. Using this setup, no endogenous skin fluorescence was detected (see Supporting Information); thus the green fluorescence comes solely from the enhancers.

*3.8. Interaction of NBD-labeled enhancers with the stratum corneum lipids*

The above results confirmed that not only the effects of enhancers on fluorescent compounds but also the fluorescent enhancers themselves can be directly visualized in the skin. Both inactive (NBD-acid) and active (NBD-C8 ester) enhancers were localized mostly in the *stratum corneum* lipid matrix; thus, the difference in their actions likely stems from their different interactions with these lipids. In theory, such interactions may be the following [4, 32-36]: 1) Small polar molecules may break the hydrogen bond network between the lipid polar heads. 2) Solvents, *e.g.,* ethanol

and dimethylsulfoxide may act via lipid extraction. 3) Amphiphilic enhancers are likely to be inserted into the skin lipid membranes, with their polar head in the hydrophilic part of the membrane and the hydrophobic chain protruding into the membrane's hydrophobic core. This may induce disturbance of the lipid packing, lateral fluidization of the lamellae and decrease of skin barrier resistance. 4) Some enhancers, *e.g.,* oleic acid and terpenes may, at high concentrations, form separate phases in the lamellae. These domains act as more permeable pores for polar substances.

Considering the molecular structures of NBD esters and NBD-acid, a plausible explanation for their different action is related to the latter two points. To support this assumption, we probed the interactions of NBD-acid and NBD-C8 ester with isolated human *stratum corneum* by FTIR (Figure 8). The control solvent, PG/W, changed keratin conformation from almost exclusively α-helices to some β-sheets, as suggested by a decrease in the ratio of the relative area of the components of the Amide I vibration at 1650 $cm^{-1}$ and 1620 $cm^{-1}$, respectively [37]. Neither NBD-acid nor NBD-C8 ester caused any changes in protein conformation after 24-h treatment of *stratum corneum* compared with the conformation observed for the control (PG/W). In contrast, NBD-C8 ester induced significant changes in the methylene symmetric stretching vibration, which originates mainly from the *stratum corneum* lipids and is sensitive to the conformation of the lipid chains. The wavenumber of the methylene symmetric stretching mode in the fully hydrated human *stratum corneum* was 2848.6 $cm^{-1}$, which indicates well-ordered lipid chains with prevailing *all-trans* conformers [38]. Treatment of the human *stratum corneum* with PG/W or NBD-acid did not induce any lipid changes. In contrast, NBD-C8 ester significantly broadened this band and shifted it to 2850.5 $cm^{-1}$ (Figure 8), which suggest incorporation of *gauche* defects into the lipid chains [38].

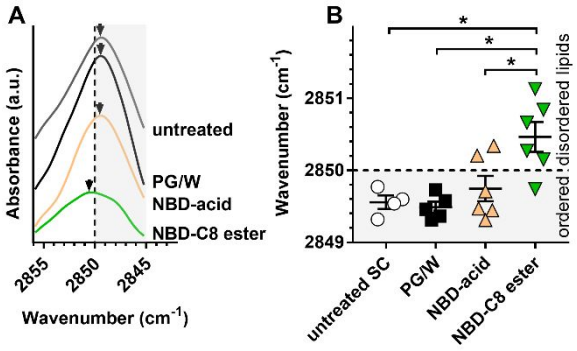


**Figure 8.** FTIR spectroscopy of isolated human *stratum corneum* treated with compound PG/W, NBD acid in PG/W and NBD-C8 ester in PG/W showing decreased conformational order of *stratum corneum* lipids (example spectra in panel A) as indicated by the higher values of symmetric methylene stretching (panel B). * statistically significant differences as indicated at $p < 0.05$ (mean ± SEM; n = 6).

A plausible explanation of this observation is that NBD ester, unlike NBD acid, is lipophilic enough to be inserted into the lipid membranes. However, the ester chains are shorter than the chains in the *stratum corneum* ceramides or fatty acids, which would disturb the lipid packing in their vicinity [4, 36]. Alternatively, NBD ester chains are rather disordered (as reflected by their infrared symmetric methylene stretching wavenumbers over 2854 $cm^{-1}$) and may also create separated domains that would act as more permeable shortcuts through the *stratum corneum*. Distinguishing between the lipid fluidization and fluid domain formation would require an enhancer with a deuterated chain.

*3.9. Conclusion*

The specific mechanisms involved in the enhancement of the drug diffusion through the skin barrier, the fate of an enhancer in the skin, and the design principles of potent and safe enhancers are not fully understood. We designed and synthesized NBD-labeled enhancers and demonstrated that the fluorescent tag does not prevent these amphiphiles from acting as permeation enhancers. Using HPLC with fluorescent detection, we distinguished between the parent enhancer and its hydrolysis product: No NBD esters were detected in the acceptor buffer, but their hydrolysis product, NBD acid, was detected, whereas both acid and esters were found in the skin. The enhancer hydrolysis occurred in the lower *stratum corneum* and epidermis, and the more hydrophilic NBD-acid, which is inactive as an enhancer, likely penetrated faster into deeper skin layers. Longer chain esters were less hydrolyzed than those with shorter chains. This behavior illustrates some of the design principles of biodegradable enhancers.

These results further showed that not only did enhancers influence the permeation of the drug, which is expected from an enhancer, but also the drug changed the permeation of enhancers. These drug effects on the flux and skin retention of enhancers were either positive or negative depending on the solvent used, which points to rather complex interactions among the drug, enhancer, solvent, and the skin.

Finally, active (NBD-C8 ester) and inactive (NBD-acid) enhancers were visualized in human skin by confocal laser scanning microscopy. Both compounds were found mostly in the *stratum corneum* intercellular spaces, suggesting that although both are located within the skin barrier lipids, only the active ester is able to effectively interact with the lipids, which was proved by infrared spectroscopy of enhancer-treated *stratum corneum*.

This proof-of-concept study illustrates the use of fluorescent enhancers to obtain insight into the skin penetration/permeation process; interactions among the enhancer, drug, solvent and skin;

and enhancer metabolism. Note that these fluorescent enhancers were developed as experimental tools and not for clinical use because the influence of the fluorescent tag on the enhancer properties, such as toxicity and irritation potential, is not known. However, these results further open the possibilities of investigating the enhancer absorption and metabolism *in vivo*, co-applying fluorescent enhancers with fluorescent drugs, comparing the skin pretreatment with the enhancer to the enhancer co-application with a drug, studying a chemical enhancer combined with physical enhancement methods, etc.

## ACKNOWLEDGMENTS

This work was supported by the Czech Science Foundation (16-25687J), Charles University (GAUK 88615 and SVV 260 401), and EFSA-CDN (No. CZ.02.1.01/0.0/0.0/16_019/0000841) co-funded by ERDF.

## SUPPORTING INFORMATION

NMR spectra and HPLC chromatograms of the fluorescent enhancers, and confocal laser scanning microscopy images of control skin samples (untreated and PG/W-treated).

## REFERENCES


1. Lane, M. E. Skin penetration enhancers. *Int J Pharm* **2013,** *447*, (1), 12-21.

2. Prausnitz, M. R.; Mitragotri, S.; Langer, R. Current status and future potential of transdermal drug delivery. *Nat Rev Drug Discovery* **2004,** *3*, (2), 115-124.

3. Barry, B. W. Novel mechanisms and devices to enable successful transdermal drug delivery. *European journal of pharmaceutical sciences : official journal of the European Federation for Pharmaceutical Sciences* **2001,** *14*, (2), 101-114.

4. Vavrova, K.; Zbytovska, J.; Hrabalek, A. Amphiphilic transdermal permeation enhancers: structure-activity relationships. *Curr Med Chem* **2005,** *12*, (19), 2273-2291.

5. Benson, H. A. Transdermal drug delivery: penetration enhancement techniques. *Curr Drug Deliv* **2005,** *2*, (1), 23-33.

6. Williams, A. C.; Barry, B. W. Penetration enhancers. *Adv Drug Deliv Rev* **2012,** *64*, 128-137.

7. Barry, B. W. Action of skin penetration enhancers-the Lipid Protein Partitioning theory. *Int J Cosmet Sci* **1988,** *10*, (6), 281-93.

8. Seto, J. E.; Polat, B. E.; VanVeller, B.; Lopez, R. F.; Langer, R.; Blankschtein, D. Fluorescent penetration enhancers for transdermal applications. *J Control Release* **2012,** *158*, (1), 85-92.

9. Novotný, J.; Kovaříková, P.; Novotný, M.; Janůšová, B.; Hrabálek, A.; Vávrová, K. Dimethylamino acid esters as biodegradable and reversible transdermal permeation enhancers: effects of linking chain length, chirality and polyfluorination. *Pharm Res* **2009,** *26*, (4), 811-821.

10. Vávrová, K.; Lorencová, K.; Novotný, J.; Holý, A.; Hrabálek, A. Permeation enhancer dodecyl 6-(dimethylamino) hexanoate increases transdermal and topical delivery of adefovir: influence of pH, ion-pairing and skin species. *Eur J Pharm Biopharm* **2008,** *70*, (3), 901-907.

11. Diblíková, D.; Kopečná, M.; Školová, B.; Krečmerová, M.; Roh, J.; Hrabálek, A.; Vávrová, K. Transdermal delivery and cutaneous targeting of antivirals using a penetration enhancer and lysolipid prodrugs. *Pharm Res* **2014,** *31*, (4), 1071-1081.

12. Chattopadhyay, A. Chemistry and biology of N-(7-nitrobenz-2-oxa-1, 3-diazol-4-yl)-labeled lipids: fluorescent probes of biological and model membranes. *Chem Phys Lipids* **1990,** *53*, (1), 1-15.

13. Novotný, J.; Pospěchová, K.; Hrabálek, A.; Čáp, R.; Vávrová, K. Synthesis of fluorescent c 24-ceramide: evidence for acyl chain length dependent differences in penetration of exogenous NBD-ceramides into human skin. *Bioorg Med Chem Lett* **2009,** *19*, (24), 6975-6977.

14. Kopečná, M.; Macháček, M.; Prchalová, E.; Štěpánek, P.; Drašar, P.; Kotora, M.; Vávrová, K. Galactosyl Pentadecene Reversibly Enhances Transdermal and Topical Drug Delivery. *Pharm Res* **2017,** *34*, (10), 2097-2108.

15. Kligman, A. M.; Christophers, E. Preparation of isolated sheets of human stratum corneum. *Arch Dermatol* **1963,** *88*, (6), 702-705.

16. Kligman, A. M.; Christophers, E. Preparation of Isolated Sheets of Human Stratum Corneum. *Arch. Dermatol.* **1963,** *88*, 702-5.

17. Bezrouk, A.; Fiala, Z.; Kotingova, L.; Krulichova, I. S.; Kopecna, M.; Vavrova, K. SAMPA: A free software tool for skin and membrane permeation data analysis. *Toxicol In Vitro* **2017,** *44*, 361-371.

18. Nakamura, H.; Ueda, N.; Ban, H. S.; Ueno, M.; Tachikawa, S. Design and synthesis of fluorescence-labeled closo-dodecaborate lipid: its liposome formation and in vivo imaging targeting of tumors for boron neutron capture therapy. *Org Biomol Chem* **2012,** *10*, (7), 1374-1380.

19. Janůšová, B.; Školová, B.; Tükörová, K.; Wojnarová, L.; Šimůnek, T.; Mladěnka, P.; Filipský, T.; Říha, M.; Roh, J.; Palát, K. Amino acid derivatives as transdermal permeation enhancers. *J Control Release* **2013,** *165*, (2), 91-100.

20. Kopečná, M.; Macháček, M.; Prchalová, E.; Štěpánek, P.; Drašar, P.; Kotora, M.; Vávrová, K. Dodecyl Amino Glucoside Enhances Transdermal and Topical Drug Delivery via Reversible Interaction with Skin Barrier Lipids. *Pharm Res* **2017,** *34*, (3), 640-653.

21. Man, M.-Q.; Feingold, K. R.; Elias, P. M. Exogenous lipids influence permeability barrier recovery in acetone-treated murine skin. *Arch Dermatol* **1993,** *129*, (6), 728-738.

22. Sochorová, M.; Staňková, K.; Pullmannová, P.; Kováčik, A.; Zbytovská, J.; Vávrová, K. Permeability barrier and microstructure of skin lipid membrane models of impaired glucosylceramide processing. *Sci Rep* **2017,** *7*, (1), 6470.

23. Vavrova, K.; Hrabalek, A.; Dolezal, P.; Samalova, L.; Palat, K.; Zbytovska, J.; Holas, T.; Klimentova, J. Synthetic ceramide analogues as skin permeation enhancers: structure-activity relationships. *Bioorg Med Chem* **2003,** *11*, (24), 5381-90.

24. Findlay, G. The simple esterases of human skin. *Br J Dermatol* **1955,** *67*, (3), 83-91.

25. Beisson, F.; Aoubala, M.; Marull, S.; Moustacas-Gardies, A.-M.; Voultoury, R.; Verger, R.; Arondel, V. Use of the tape stripping technique for directly quantifying esterase activities in human stratum corneum. *Anal Biochem* **2001,** *290*, (2), 179-185.

26. Lau, W. M.; Ng, K. W.; Sakenyte, K.; Heard, C. M. Distribution of esterase activity in porcine ear skin, and the effects of freezing and heat separation. *Int J Pharm* **2012,** *433*, (1-2), 10-15.

27. Wang, T.-Y.; Silvius, J. R. Different sphingolipids show differential partitioning into sphingolipid/cholesterol-rich domains in lipid bilayers. *Biophys J* **2000,** *79*, (3), 1478-1489.

28. Pagano, R. E.; Sleight, R. G. Defining lipid transport pathways in animal cells. *Science* **1985,** *229*, 1051-1058.

29. Alvarez-Román, R.; Naik, A.; Kalia, Y.; Fessi, H.; Guy, R. H. Visualization of skin penetration using confocal laser scanning microscopy. *Eur J Pharm Biopharm* **2004,** *58*, (2), 301-316.

30. Liu, X.; Quan, P.; Li, S.; Liu, C.; Zhao, Y.; Zhao, Y.; Fang, L. Time dependence of the enhancement effect of chemical enhancers: Molecular mechanisms of enhancing kinetics. *J Control Release* **2017,** *248*, 33-44.

31. Grams, Y. Y.; Alaruikka, S.; Lashley, L.; Caussin, J.; Whitehead, L.; Bouwstra, J. A. Permeant lipophilicity and vehicle composition influence accumulation of dyes in hair follicles of human skin. *European journal of pharmaceutical sciences : official journal of the European Federation for Pharmaceutical Sciences* **2003,** *18*, (5), 329-336.

32. Smith, E. W.; Maibach, H. I., *Percutaneous penetration enhancers*. CRC Press: 1995.

33. Dragicevic, N.; Maibach, H. I., *Percutaneous Penetration Enhancers Chemical Methods in Penetration Enhancement: Modification of the Stratum Corneum*. Springer: 2015.

34. Moser, K.; Kriwet, K.; Naik, A.; Kalia, Y. N.; Guy, R. H. Passive skin penetration enhancement and its quantification in vitro. *Eur J Pharm Biopharm* **2001,** *52*, (2), 103-112.

35. Ongpipattanakul, B.; Burnette, R. R.; Potts, R. O.; Francoeur, M. L. Evidence that oleic acid exists in a separate phase within stratum corneum lipids. *Pharm Res* **1991,** *8*, (3), 350-354.

36. Pham, Q. D.; Björklund, S.; Engblom, J.; Topgaard, D.; Sparr, E. Chemical penetration enhancers in stratum corneum—Relation between molecular effects and barrier function. *J Control Release* **2016,** *232*, 175-187.

37. Bernard, G.; Auger, M.; Soucy, J.; Pouliot, R. Physical characterization of the stratum corneum of an in vitro psoriatic skin model by ATR-FTIR and Raman spectroscopies. *Biochim. Biophys. Acta* **2007,** *1770*, (9), 1317-1323.

38. Mendelsohn, R.; Flach, C. R.; Moore, D. J. Determination of molecular conformation and permeation in skin via IR spectroscopy, microscopy, and imaging. *Biochim. Biophys. Acta* **2006,** *1758*, (7), 923-33.

**Table of Contents graphic**

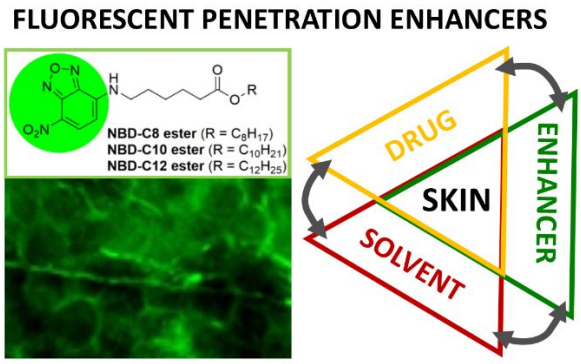

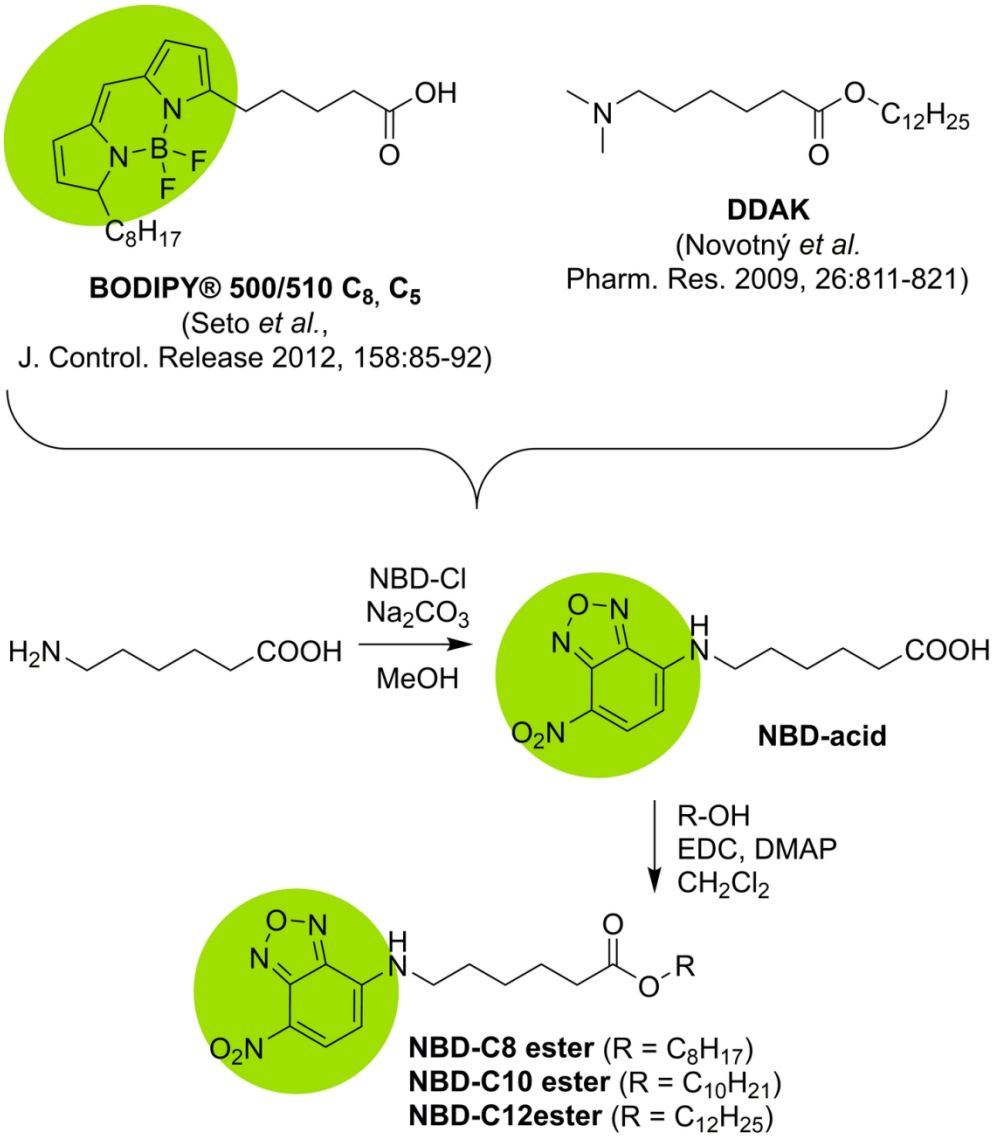


122x139mm (300 x 300 DPI)

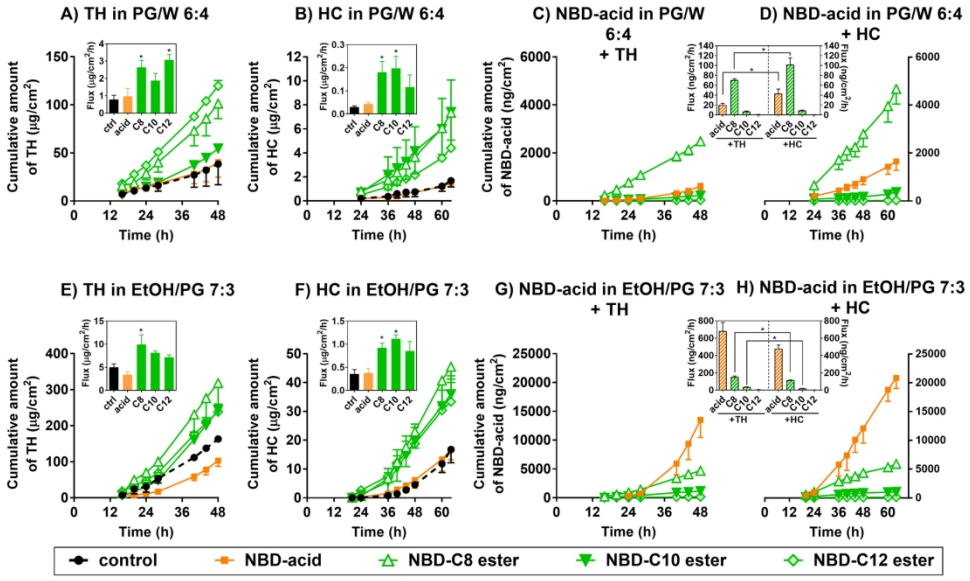


169x100mm (300 x 300 DPI)

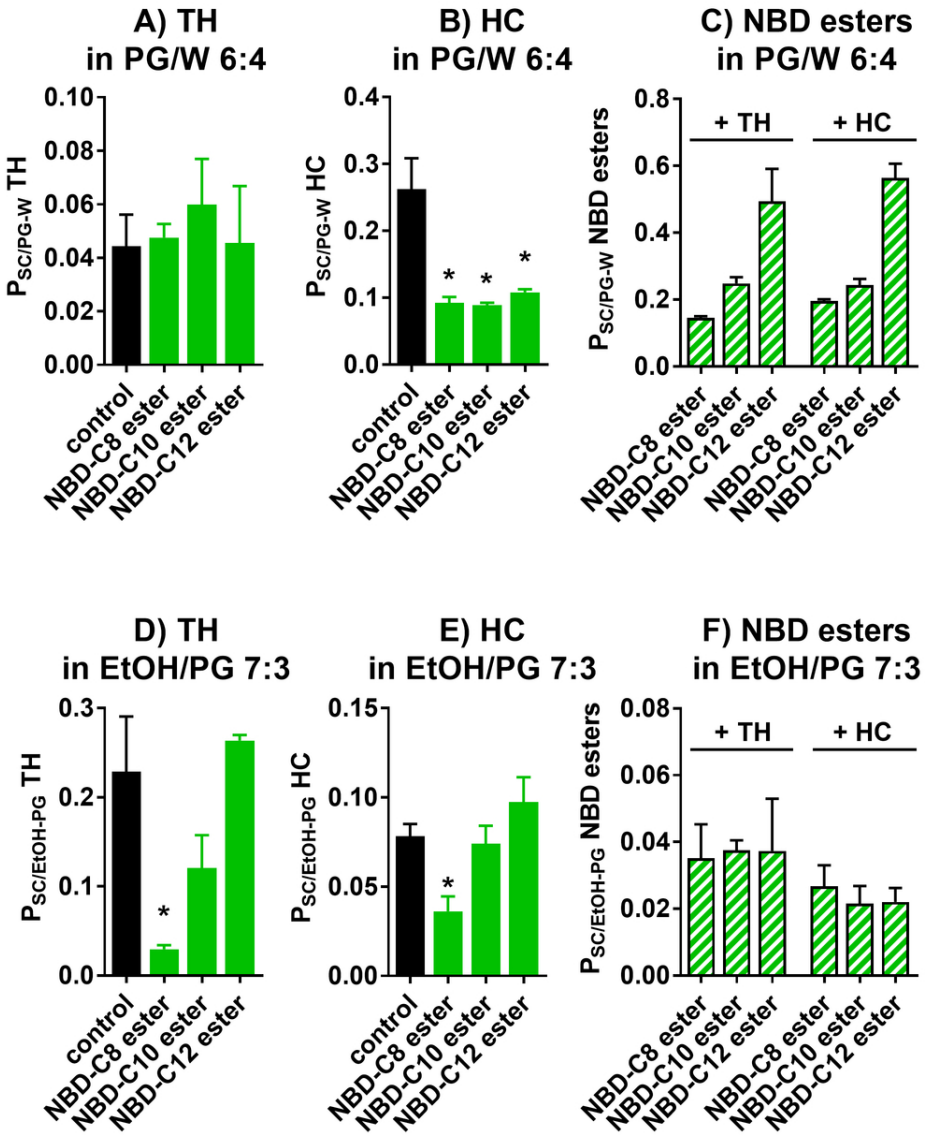


90x108mm (300 x 300 DPI)

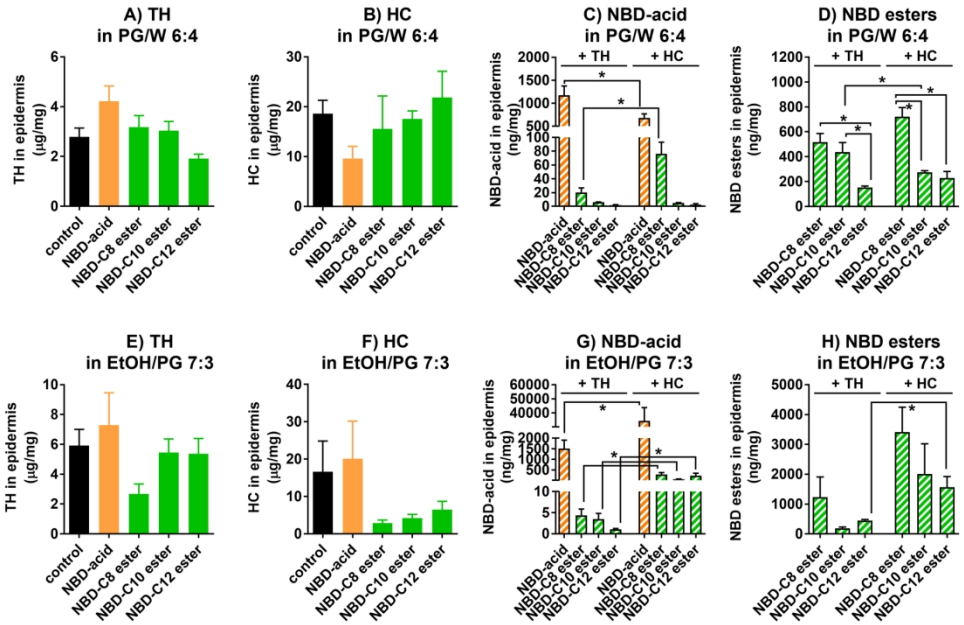


169x111mm (300 x 300 DPI)

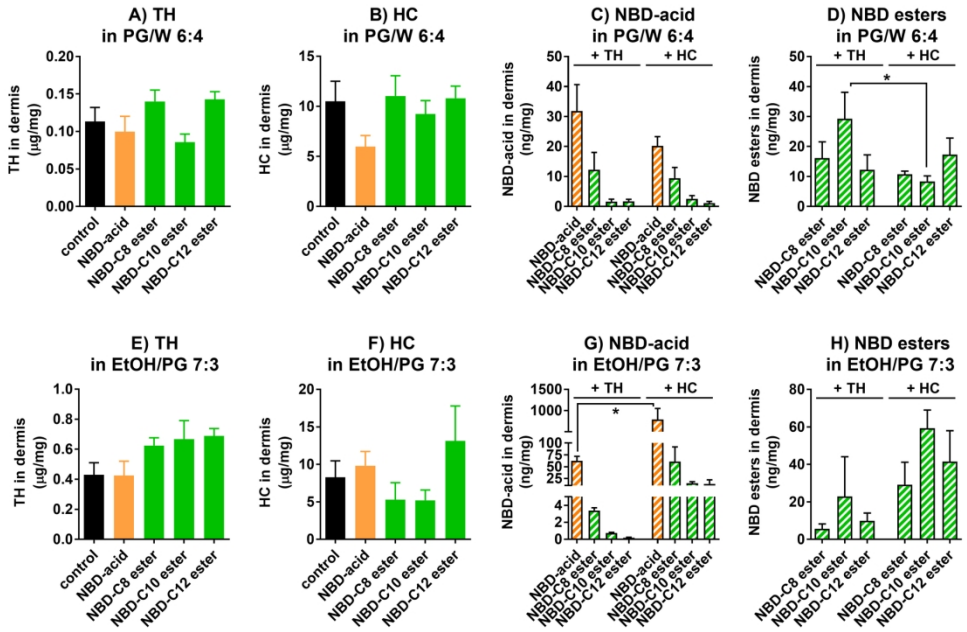


169x112mm (300 x 300 DPI)

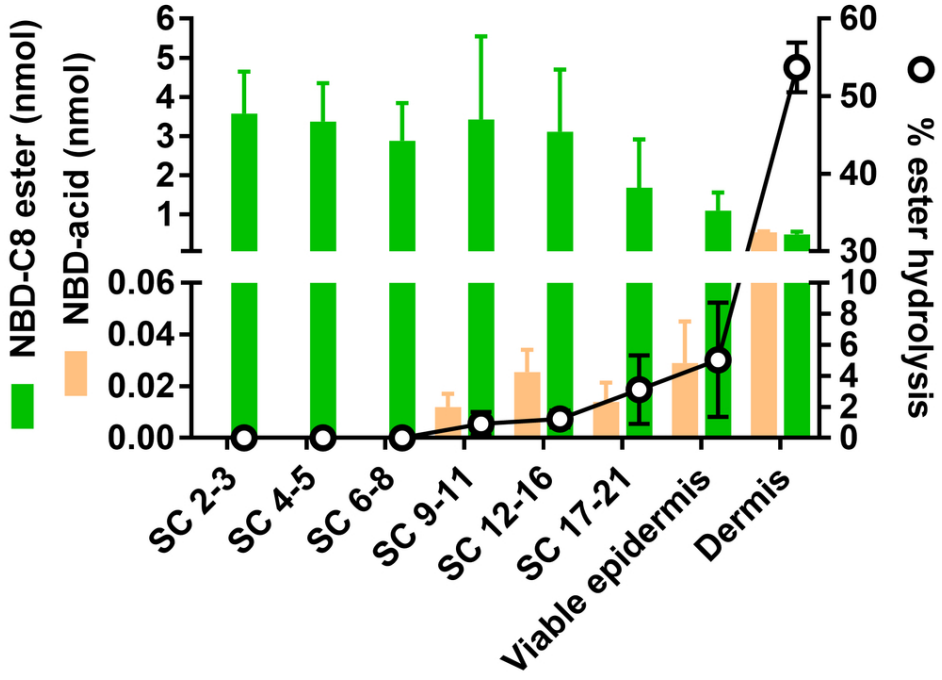


89x67mm (300 x 300 DPI)

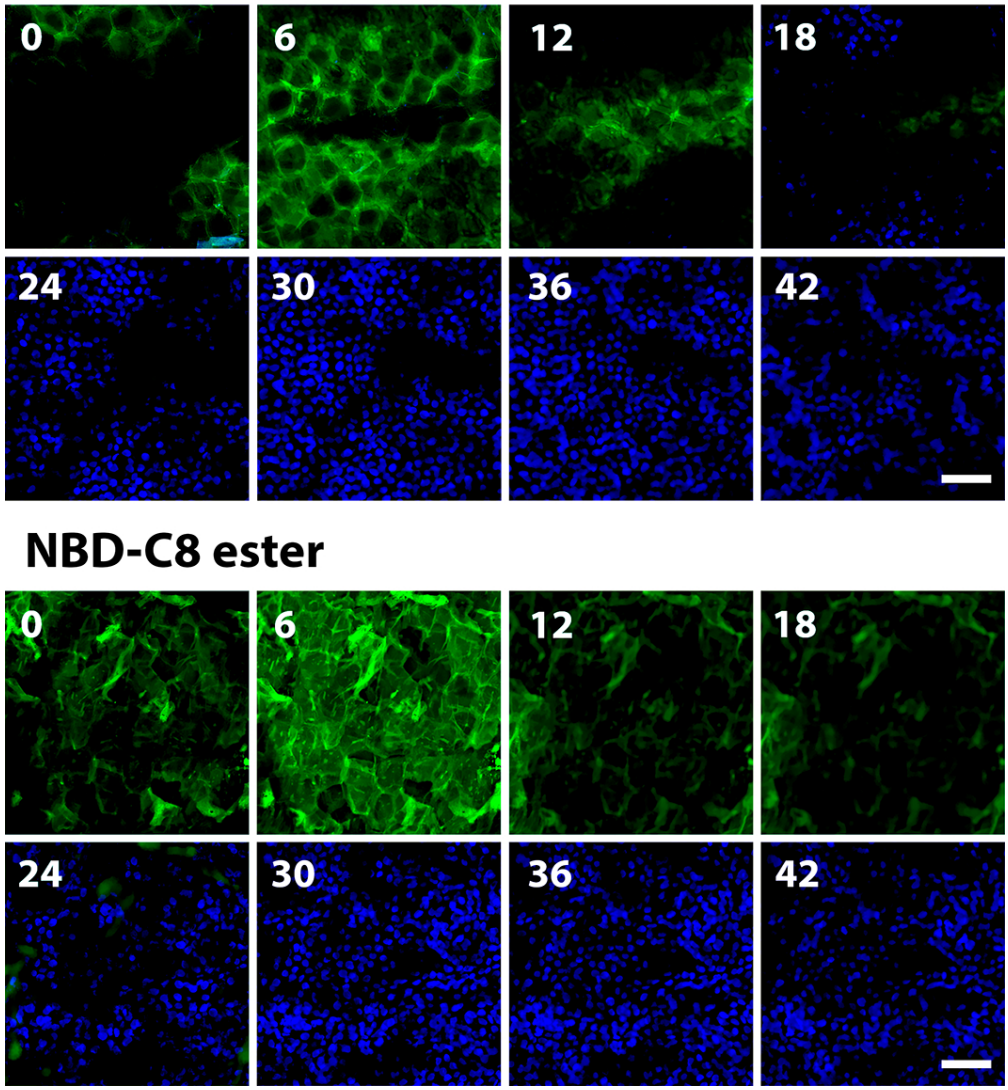
NBD-acid
0
6
12
18
24
30
36
42
NBD-C8 ester
0
6
12
18
24
30
36
42

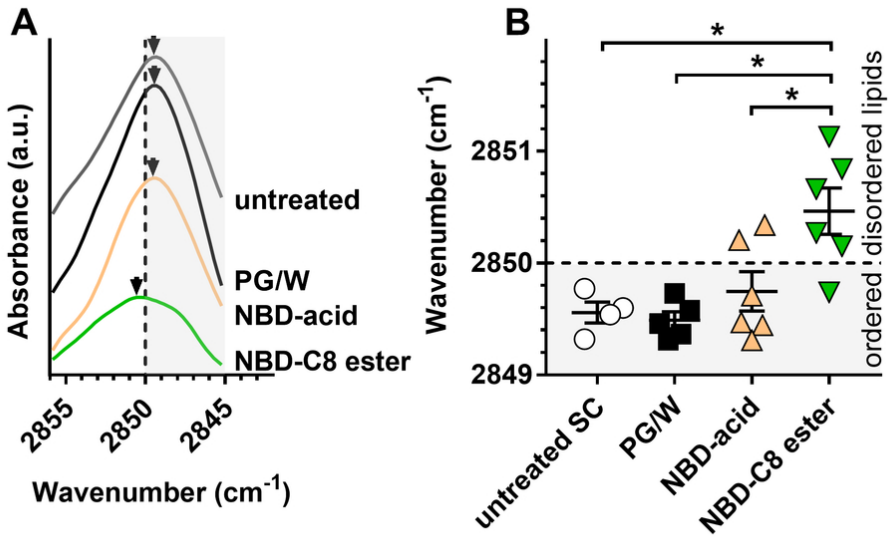


84x52mm (300 x 300 DPI)

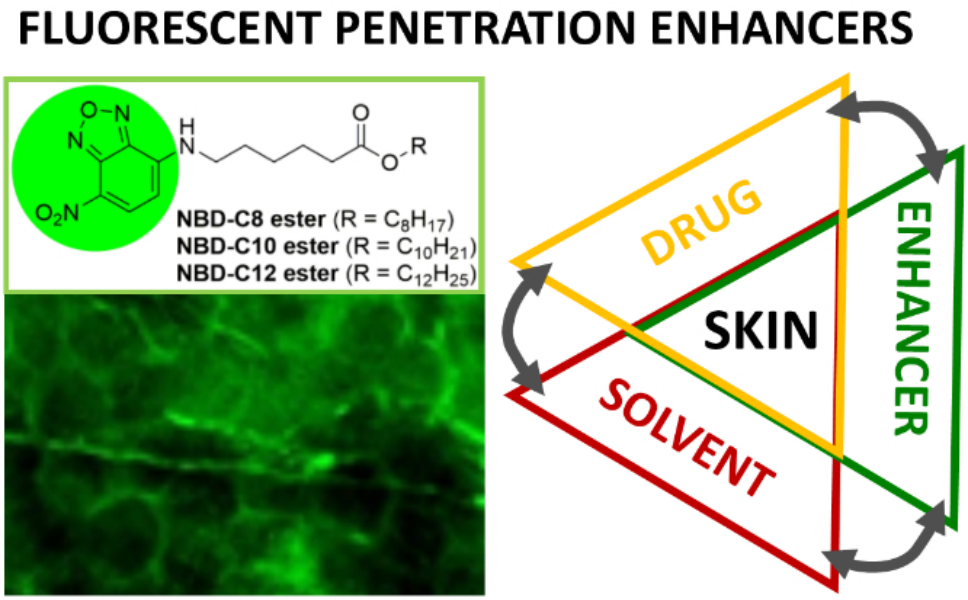


TOC graphic

182x114mm (96 x 96 DPI)